FOSSIL ENERGY

DOE/BC/15111-4
(OSTI ID: 792020)

# RESPONSIVE COPOLYMERS FOR ENHANCED PETROLEUM RECOVERY

Final Report
September 29, 1998-September 28, 2001

By:
Charles McCormick
Roger Hester

Date Published: February 2002

Work Performed Under Contract No. DE-AC26-98BC15111

University of Southern Mississippi
Hattiesburg, Mississippi

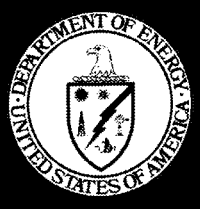


**National Energy Technology Laboratory**
**National Petroleum Technology Office**
**U.S. DEPARTMENT OF ENERGY**
**Tulsa, Oklahoma**

DOE/BC/15111-4
Distribution Category UC-122

# Responsive Copolymers for Enhanced Petroleum Recovery

By
Charles McCormick
Roger Hester

February 2002

Work Performed Under DE-AC26-98BC15111

Prepared for
U.S. Department of Energy
Assistant Secretary for Fossil Energy

Jerry Casteel, Project Manager
National Petroleum Technology Office
P.O. Box 3628
Tulsa, OK 74101

Prepared by
University of Southern Mississippi
Department of Polymer Science
Box 5157
Hattiesburg, MS 39406

**TABLE OF CONTENTS**

CHAPTER EIGHT



LIST OF TABLES



LIST OF FIGURES

LIST OF SCHEMES

## ABSTRACT

A coordinated research program has been initiated with the aim of developing environmentally responsive copolymers for Improved Oil Recovery (IOR). These novel polymer systems possess amphipathic microstructures which allow reversible pH-, salt, shear-, or temperature-responsiveness in aqueous media. Viscosity, fluid flow behavior, polymer interactions with reservoir rock and entrapped oil, and phase behavior can be changed by altering pH or salt concentration or by adjusting flow rates. The objectives of this work are to: synthesize responsive, amphiphilic systems; characterize molecular structure and solution behavior; measure rheological properties of the aqueous fluids including behavior in fixed geometry flow profiles and beds; and to tailor polymer compositions for *in situ* rheology control under simulated reservoir conditions. This report focuses on the synthesis, characterization and solution properties of terpolymers of sodium acrylate, acrylamide, and the zwitterionic monomer 4-(2-acrylamido-2-methylpropylidmethylammonio)butanoate as well as electrolyte and pH-responsive zwitterionic copolymers of 4-(2-acrylamido-2-methylpropylidmethyl-ammonio)butanoate with 3-(2-acrylamido-2-methylpropyldimethylammonio) propanesulfonate. Also reported is the design and operation of a capillary rheometer for determining solution viscosities at elevated temperatures.

## SUMMARY: BACKGROUND, OBJECTIVES, AND OVERVIEW OF RESEARCH DURING FY 2001

Introduction

A coordinated research program has been initiated with the aim of developing environmentally responsive copolymers for Improved Oil Recovery (IOR). These novel polymer systems possess amphipathic microstructures which allow reversible pH-, salt, shear-, or temperature-responsiveness in aqueous media. Conformational reordering in response to such controllable variables can result in substantial changes in viscosity and phase behavior. These characteristics are of potential utility in controlling both fluid mobility and conformance, particularly for *in situ* processes. Responsive polymers have attributes that should overcome limitations inherent in even the best conventional IOR polymers. Salt- and pH "triggers" strategically placed along the macromolecular backbone determine hydrodynamic volume and, thus, rheological behavior. Viscosity, fluid flow behavior, polymer interactions with reservoir rock and entrapped oil, and phase behavior can be changed by altering pH or salt concentration or by adjusting flow rates. Polymers are targeted to act alone or with surfactant to significantly alter fluid flow through porous media. Both viscosity of the fluid and permeability of the substrate to the aqueous phase can, in principle, be altered.

Research Objectives

The objectives of this work are to: synthesize responsive, amphiphilic systems; characterize molecular structure and solution behavior; measure rheological properties of the aqueous fluids including behavior in fixed geometry flow profiles and beds; and to tailor final polymer compositions for *in situ* rheology control under simulated reservoir conditions.

Responsive Polymers: Synthesis, Characterization, and Behavior in Aqueous Media

Water-soluble polymers incorporating both anionically and cationically charged species are the subject of increasing interest in numerous academic and industrial laboratories. Polyampholytes, as they have been termed, exhibit distinctive rheological behavior, which is potentially useful in a number of commercial applications such as enhanced oil recovery, drag reduction, personal care formulations, and water remediation. Of particular interest is the possibility of viscosity maintenance or increase of polyampholyte solutions in the presence of electrolytes and surfactants.

Polyampholytes have been synthesized by copolymerization of both anionic and cationic monomers into the polymer backbone[1-13] or by incorporating into the polymer zwitterionic monomer units.[14-23] The incorporation of nonionic, hydrophilic comonomers is often necessary to impart solubility and offers a convenient way of altering charge density.[24-30] An interesting feature of low-charge density polyampholytes is the tendency to form intermolecular associations in deionized water. Besides possessing unique molecular architecture, polyampholytes can exhibit pH responsiveness, which is especially important for developing "smart' rheological fluids.

Chapter 2 reports that terpolymers of sodium acrylate (NaA), acrylamide (AM), and the zwitterionic monomer 4-(2-acrylamido-2-methylpropanedimethylammonio) butanoate (AMPDAB) were prepared by free radical polymerization in 0.5 M NaBr aqueous solution using potassium persulfate as the initiator. The feed ratio of AMPDAB : NaA : AM was varied from 5 : 5 : 90 to 40 : 40 : 20 mol%, with the total monomer concentration held constant at 0.45 M.

Terpolymer compositions were determinedy by $^{13}C$ NMR. Molecular weights varied from 3.0 X $10^6$ to 9.7 X $10^6$ g/mol.

The solution behavior of terpolymers of sodium acrylate (NaA), acrylamide (AM), and the zwitterionic monomer 4-(2-acrylamido-2-methylpropanedimethylammonio) butanoate (AMPDAB) was analyzed and the results reported in Chapter 3.. All terpolymers were soluble in deionized water and salt solutions at all pH values. The dilute and semidilute solution behavior of the terpolymers was studied as a function of composition, pH, and added electrolytes. Polyelectrolyte behavior was observed for all terpolymers at pH 8.5, as evidenced by high viscosity values at low polymer concentrations and viscosity decrease in the presence of added electrolytes. The reduced viscosity as a function of decreasing pH exhibits a minimum as the terpolymer undergoes a polyanion/polyzwitterion/polycation transition. Comparison of the solution behavior of the terpolymers to terpolymers of 3-(2-acrylamido-2-methylpropane dimethylammonio)-1-propane sulfonate (AMPDAPS), AM, and NaA (AADPAS series) as well as copolymers of AMPDAB and AM (AMPDAB series) have been made.

In Chapter 4 we report that amphoteric copolymers of the carboxybetaine monomer 4-(2-acrylamido-2-methylpropyl dimethylammonio) butanoate (AMPDAB), **1**, with the sulfobetaine monomer 3-(2-acrylamido-2-methylpropyldimethylammonio) propanesulfonate (AMPDAPS), **2**, have been synthesized by free radical polymerization in 0.5 M NaBr. The feed ratios of **1** : **2** were varied from 100:0 to 0:100 mol%. Molecular weights were determined by low angle laser light scattering and range from 1.65 X $10^6$ to 3.95 X $10^6$ g/mol.

The solution behavior of amphoteric copolymers of the carboxybetaine monomer 4-(2-acrylamido-2-methylpropyl dimethylammonio) butanoate (AMPDAB), **1**, with the sulfobetaine monomer 3-(2-acrylamido-2-methylpropyldimethylammonio) propanesulfonate (AMPDAPS), **2**, have been investigated using turbidimetric techniques and this work is reported in Chapter 5. The homopolymer of **2** was insoluble in deionized water but soluble in aqueous solutions containing a critical concentration of added electrolytes. In contrast, the homopolymer of **1** was soluble in deionized water. The solubility behavior of copolymers of **1** and **2** is complex and varies with copolymer composition, pH, as well as the concentration and nature of the added electrolytes. Coulombic interactions and hydration effects are suggested to be the main factors affecting the solubility behavior of these amphiphilic copolymers. Low shear viscosity studies were conducted at varying electrolyte concentration and pH values. The copolymers containing higher incorporation of the AMPDAPS, **2**, mer units showed greater enhancement in viscosity with increased electrolyte concentration. Copolymers containing AMPDAB, **1**, mer units exhibit polyelectrolyte behavior at low pH in deionized water as the carboxylate groups are protonated resulting in an overall cationic charge along the polymer chain. The solution behavior of these responsive systems is rationalized based on competitive hydration of the zwitterionic moieties under testing conditions.

Characterization of Flow Behavior in Aqueous Media

Oil reservoirs have pore channels of changing geometry that produce accelerations and decelerations of any fluid forced through the reservoir. These fluid velocity variations in the flow direction produce alternating extension and compression strains within the fluid. Since polymer coils in aqueous solutions exhibit significantly more resistance to extension and compression strains compared to water, the polymer solutions that are used to flood reservoirs show a decrease in mobility that favors improved oil recovery.

Polymer coils of larger hydrodynamic volume are more effective in decreasing solution mobility in porous media. A polymer's hydrodynamic volume is proportional to the product of two measurable properties, intrinsic viscosity and molecular weight. Intrinsic viscosity increases with increased solvent-polymer thermodynamic interactions. Thus, a good candidate for mobility control in flow through porous media is a polymer that is highly solvated by the solvent at the applied conditions.

In the application of enhanced oil recovery (EOR), polymer solution temperature is elevated as it flows into the oil reservoir. Also *in situ* electrolytes will be dissolved into the polymer solution as it travels through the reservoir. The added electrolytes usually unfavorably alter polymer solvation. Ideally, a "smart" polymer used for EOR should become more solvated with increases in temperature and electrolyte concentrations. This "smart" polymer solution property would insure that fluid mobility control would not be diminished as the solution migrates through a hot reservoir and gains electrolytes. This polymer property would thereby improve sweep efficiency and oil recovery.

The degree of polymer solvation in a solution is proportional to the intrinsic viscosity of the polymer in the solution environment. Therefore to predict polymer solution mobility during reservoir flooding, it is extremely important to accurately measure polymer solution intrinsic viscosities over a range of temperature and solvent conditions encountered within typical oil reservoirs.

Chapter 6 reports the construction of a capillary tube viscometer capable of measuring the intrinsic viscosities of polymer solutions over a range of temperatures and solvent compositions that are typically found during polymer flooding of oil reservoirs. Chapter 7 reports the analytical and raw data analysis procedures required for accurate and meaningful intrinsic viscosity determinations using the capillary tube viscometer. Chapter 8 gives theoretical relationships that project polymer solution intrinsic viscosities as functions of temperature. These relationships are used to interpret solvent-macromolecule thermodynamic interactions for several acrylamide copolymers. Using the screen extensional rheometer, dilute polymer solution extensional rheological properties were measured as a function of fluid temperature and these properties were correlated with solution intrinsic viscosities.

The work reported in Chapters 6 through 8 shows that coupling information from a capillary tube viscometer and a screen extensional rheometer can project the flow behavior of polymer solution through porous media over a range of temperature conditions. These two analytical tools will be used to enhance future polymer synthesis efforts by enabling the rapid laboratory screening of many "smart" polymer macromolecular structural alterations for advantageous porous media flow properties at simulated reservoir conditions without the expense of actually flooding oil reservoirs.

# CHAPTER 2. pH RESPONSIVE BEHAVIOR OF TERPOLYMERS OF SODIUM ACRYLATE, ACRYLAMIDE, AND THE ZWITTERIONIC MONOMER 4-(2-ACRYLAMIDO-2-METHYLPROPYLDIMETHYLAMMONIO)BUTANOATE: SYNTHESIS AND CHARACTERIZATION

## INTRODUCTION

Water-soluble polymers incorporating both anionically and cationically charged species are the subject of increasing interest in numerous academic and industrial laboratories. Polyampholytes, as they have been termed, exhibit distinctive rheological behavior, which is potentially useful in a number of commercial applications such as enhanced oil recovery, drag reduction, personal care formulations, and water remediation. Of particular interest is the possibility of viscosity maintenance or increase of polyampholyte solutions in the presence of electrolytes and surfactants.

Polyampholytes have been synthesized by copolymerization of both anionic and cationic monomers into the polymer backbone[1-13] or by incorporating into the polymer zwitterionic monomer units.[14-23] The incorporation of nonionic, hydrophilic comonomers is often necessary to impart solubility and offers a convenient way of altering charge density.[24-30] An interesting feature of low-charge density polyampholytes is the tendency to form intermolecular associations in deionized water. Besides possessing unique molecular architecture, polyampholytes can exhibit pH responsiveness, which is especially important for developing "smart' rheological fluids.

Recently, we inititated studies on polyampholytes incorporating such pH responsive species. These systems can behave as polyelectrolytes or polyampholytes, depending on the pH of the environment. [30,31] In addition, we introduced a novel way of preparing polyampholytes with a charge imbalance (the AADAPS series) by incorporating the sulfobetaine monomer 3-(2-acrylamido-2-methylpropanedimethy-lammonio) propanesulfonate (AMPDAPS), acrylamide (AM), and sodium acrylate (NaA).[32] At high pH, the solution behavior was dictated by the excess charge provided by the sodium acrylate units. Furthermore, enhanced viscosity was observed for the AADAPS termpolymers in the presence of electrolytes compared to copolymers of AM and NaA and copolymers of AM and AMPDAPS. At low pH, the solution viscosity was dramatically reduced due to the coulombic attractions between the sulfobetaine units as well as hydrogen bonding effects between the acrylic acid and acrylamido mer units. In continuation of this theme, we report in this article the synthesis and solution behavior of similar terpolymers based on the carboxybetaine monomer, 4-(2-acrylamido-2-methylpropanedimethyl ammonio)butanoate (AMPDAB). In contrast to the sulfobetaine monomer AMPDAPS, AMPDAB provides a pH trigger that allows this system to be polyanionic, polyzwitterionic, or polycationic, depending on the pH of the aqueous medium.

## EXPERIMENTAL

### Materials

Acrylamide (AM) from Aldrich was recrystallized twice from acetone and vacuum dried at room temperature. Acrylic acid (AA) from Aldrich was vacuum distilled prior to use. 4-(2-

Acrylamido-2-methylpropanedimethyl ammonio)butanoate (AMPDAB) was synthesized by the quaternization reaction of 2-acrylamido-2-methylpropanedimethyl amine with ethyl 4-bromobutyrate followed by hydrolysis of the ester functionality as previously reported.[7] Potassium persulfate from J. T. Baker was recrystallized twice from deionized water. All other materials were used as received.

**Synthesis of Terpolymers of 4-(2-Acrylamido-2-methylpropanedimethyl ammonio) Butanoate, Acrylamide, and Sodium Acrylate**

The terpolymers of AMPDAB, AM, and NaA (the AADAB series) were synthesized by free radical polymerization in a 0.5 M aqueous NaBr solution under nitrogen at 30 °C using 0.1 mol % potassium persulfate as the initiator at pH 8. The feed ratio of AMPDAB : NaA : AM was varied from 5 : 5 : 90 to 40 : 40 : 20 mol % with the total monomer concentration held constant at 0.45 M.

In a typical synthesis, specified quantities of the monomers were dissolved in a designated volume of deionized water. To this solution was added one equivalent of sodium hydroxide per equivalent of AMPDAB and NaA and the pH adjusted to 8.5. The necessary quantity of NaBr was then added to achieve a 0.5 M NaBr solution. The reaction mixture was sparged with nitrogen and initiated with 0.1 mol % potassium persulfate (based on total monomer concentration). The reaction was terminated near 50 % conversion due to the high viscosity of the reaction medium and as a precaution against copolymer drift. The copolymers were precipitated in acetone, dissolved in deionized water, then dialyzed against deionized water using Spectra/Por No. 4 dialysis bags with molecular weight cutoffs of 12,000 to 14,000 g/mol. After dialyzing for 9 days, the copolymers were isolated by lyophilization.

**Synthesis of the Copolymer of Acrylamide with 4-(2-Acrylamido-2-methyl propanedimethyl ammonio)Butanoate**

The polymerization procedure for preparing the copolymer of AMPDAB and AM was conducted in a manner similar to that for AADAB as previously reported.[7]

**Synthesis of Terpolymers of 3-(2-Acrylamido-2-Methylpropanedimethyl ammonio)Propanesulfonate, Acrylamide, and Acrylic Acid**

The terpolymers of AMPDAPS, AM, and NaA (the AADAPS series) were synthesized by free radical polymerization in a 0.5 M aqueous NaCl solution under nitrogen at 30 °C using 0.1 mol % potassium persulfate as the initiator at pH 8. The procedure has been previously reported.[8]

**Copolymer Characterization**

$^{13}C$ NMR spectra of the polymers were obtained at 50.3 MHz with a Bruker AC 200 spectrometer using 10-15 wt % 0.5 M NaCl ($D_2O$) polymer solutions with 3-(trimethylsilyl)-1-propane-sulfonic acid, sodium salt (DSS) as a reference. A recycle delay of 6 s, 90° pulse length, and gated decoupling to remove all NOE were used for quantitative spectral analysis. Integration of the amido carbonyl resonance of AMPDAB, the carboxylate carbonyl resonance of NaA, and the resonances from both the amido carbonyl of AM and the carboxylate carbonyl of AMPDAB were used to determine terpolymer compositions to within ± 6 % of the reported values. Refractive index increments were obtained using a Chromatix KMX-16 laser differential

refractometer. Molecular weight studies were performed with a Chromatix KMX-6 low-angle laser light scattering instrument at 25 °C. Polymer solutions for light scattering ($C_p$ = 2 X $10^{-4}$ g/mL) in 1.0 M NaCl at pH 8 were aged to ensure complete dissolution and subsequently filtered through Millipore 0.45 μm filters to remove dust; dilutions were prepared with filtered 1.0 M NaCl.

## RESULTS AND DISCUSSION

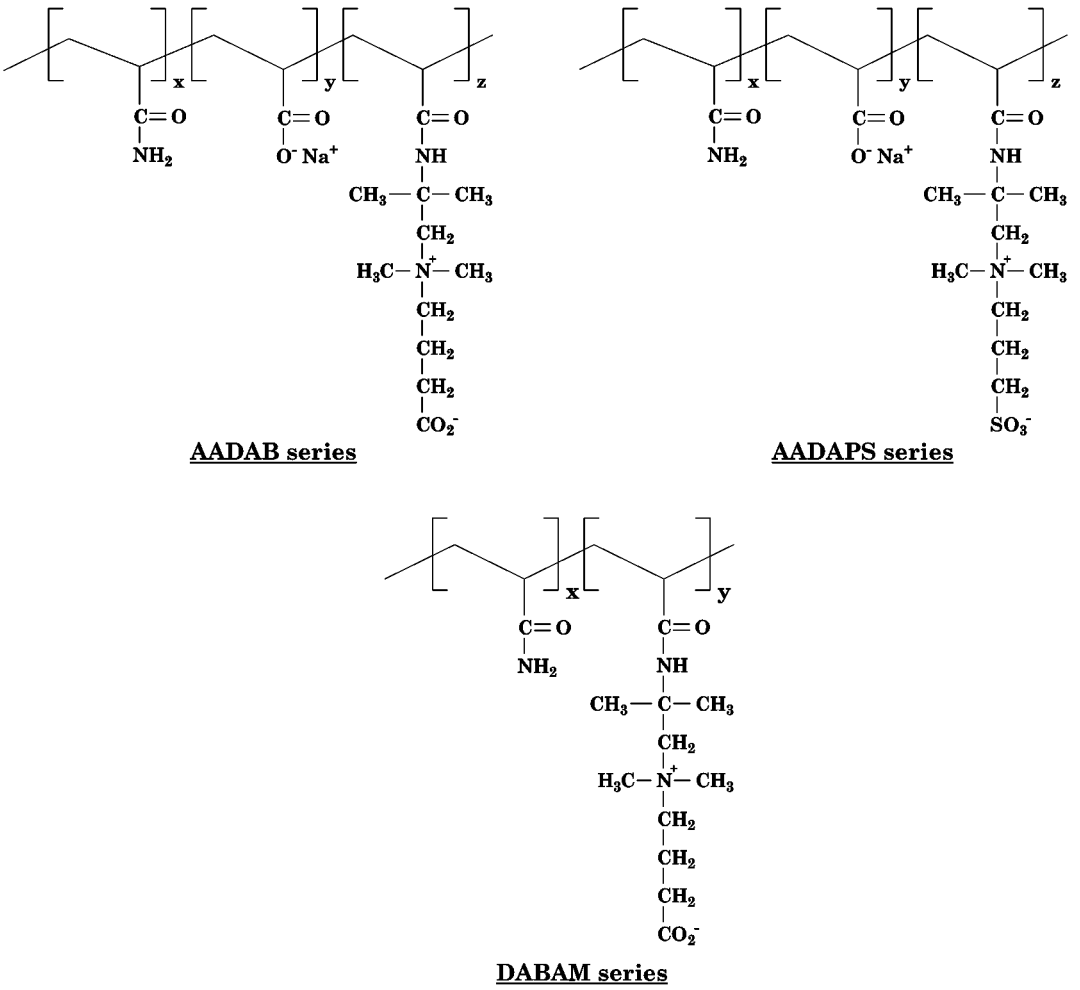


**Figure 2.1.** Structural composition of the AADAB, AADAPS, and DABAM series.

### Compositional Analysis

The terpolymers of AMPDAB, AM, and NaA (the AADAB series) were synthesized by varying the feed ratios of AMPDAB : NaA : AM from 5 : 5 : 90 to 40 : 40 : 20 mol %. Copolymers of AMPDAB and AM (the DABAM series) and terpolymers of AMPDAPS, AM, and NaA (the AADAPS series) were synthesized previously.[31,32] The terpolymer series reported in this article are shown in Figure 1. The terpolymer compositions were determined from $^{13}C$ NMR spectroscopy by integration of the carbonyl resonances. Monomer distribution will be affected by the degree of conversion; however, previous studies in our laboratories on similar

types of monomers have suggested no substantial drift at low to moderate monomer conversions. The terpolymer compositions presented in this article do not suggest a major depletion of any of the monomers during the course of polymerization that may cause a significant drift in composition at 50 % conversion to polymer. AMPDAB and AM incorporation in both the AADAB and DABAM series approximates the feed compositions, indicating similar reactivities of the respective monomers. NaA incorporation in the AADAB series was found to be lower than the feed composition, indicating higher reactivity of the acrylamido-type monomers. The reaction parameters and the resulting terpolymer compositions are given in Table 1.

**Table 2.1. Reaction Parameters for the AADAB, AADAPS, and DABAM series.**

| Sample | Feed ratio (mol %) (X/Y/Z) | AMPDAB found[a] (mol %) | AM found[a] (mol %) | NaA found[a] (mol %) | AMPDAPS found[a] (mol %) |
|---|---|---|---|---|---|
| AADAB-5 | 90/5/5 | 5.5 | 91.2 | 3.3 | - |
| AADAB-10 | 80/10/10 | 10 | 83.7 | 6.3 | - |
| AADAB-25 | 50/25/25 | 27.2 | 54.5 | 18.3 | - |
| AADAB-40 | 20/40/40 | 48.1 | 17.0 | 34.9 | - |
| AADAPS-10 | 80/10/10 | - | 85.2 | 4.6 | 10.2 |
| AADAPS-40 | 20/40/40 | - | 24.2 | 25.4 | 50.4 |
| DABAM-40 | 60/40 | 40.7 | 59.3 | - | - |

[a] Determined by $^{13}C$ NMR spectroscopy.

**Low-Angle Laser Light Scattering**

Weight-average molecular weights were determined by classical low-angle laser light scattering. Table 2 shows the data obtained at 20 °C in 1.0 M NaCl at pH 8. The solvent system was chosen to ensure complete screening of the ionic charges incorporated into the terpolymers. The molecular weights vary from $3.0 \times 10^6$ to $9.7 \times 10^6$ g/mol for the AADAB series. Second virial coefficients ($A_2$) were also determined, and the values obtained are higher than those found for the AADAPS series. This is likely a result of the more hydrophilic nature of the carboxybetaine mer units compared to the sulfobetaine units.[9,10] Furthermore, the sodium acrylate mer units enhance hydration, as noted by the observation that the $A_2$ value for AADAB-40 is approximately five times greater than that for DABAM-40.

**Table 2.2. Classical Light-Scattering Data for the AADAB, AADAPS, and DABAM series.**

| Sample | Zwitterionic monomer found[a] (mol %) | $M_w \times 10^{-6}$ (g/mol) | $A_2 \times 10^4$ (ml · mol /g$^2$) | DP $\times 10^{-4}$ |
|---|---|---|---|---|
| AADAB-5 | 5.5[b] | 4.2 | 3.37 | 5.1 |
| AADAB-10 | 10.0[b] | 5.5 | 17.0 | 6.0 |
| AADAB-25 | 27.2[b] | 9.7 | 7.40 | 7.7 |
| AADAB-40 | 48.0[b] | 3.0 | 3.12 | 1.8 |
| AADAPS-10 | 10.2[c] | 5.4 | 2.95 | 5.7 |
| AADAPS-40 | 50.4[c] | 4.7 | 2.23 | 2.5 |
| DABAM-40 | 40.7[b] | 9.8 | 0.60 | 6.7 |

[a] Determined by $^{13}$C NMR spectroscopy.
[b] mol % AMPDAB found.
[c] mol % AMPDAPS found.

## CONCLUSION

The AADAB series, consisting of terpolymers of NaA, AM, and the carboxybetaine monomer, AMPDAB, have been prepared by free radical polymerization in 0.5 M aqueous NaBr solution using potassium persulfate as the initiator. Copolymer compositional studies by $^{13}$C NMR indicate a preference for acrylamido monomer incorporation. Molecular weights range from 3.0 to 9.7 $\times$ 10$^6$ g/mol, as determined by low-angle laser light scattering. All terpolymers are soluble in deionized water, although AADAB-10 and –25 require longer dissolution times. In ongoing work, the AADAB, AADAPS, and DABAM series will be compared to determine the effects of the nature of the zwitterionic mer unit and the incorporation of NaA on solution behavior. Viscosimetric studies will be performed to evaluate the effects of polymer concentration, added electrolytes, and solution pH on each polymer series.

## REFERENCES


1. McCormick, C. L. and Johnson, C. B. *Macromolecules*, **21**, 687 (1988).
2. McCormick, C. L. and Johnson, C. B. *Macromolecules*, **21**, 694 (1988).
3. C. L. McCormick and L. C. Salazar, *Macromolecules* **25**, 1896 (1992).
4. T. Alfrey and H. Morawetz, *J. Am. Chem. Soc., 74*, **436** (1952).
5. T. Alfrey, R. Fuoss, H. Morawetz, and S. H. Pinner, *J. Am. Chem. Soc.,* **74**, 438 (1952).
6. T. Alfrey and S. H. Pinner, *J. Polym. Sci.,* **23**, 533 (1957).
7. D.O. Jordan and T. Kuruscev, *Polymer,* **1**, 185 (1960).
8. G. Ehrlich and P. Doty, *J. Am. Chem. Soc.,* **76**, 3764 (1954).
9. A. Katchalsky and I. R. Miller, *J. Polym. Sci.,* **13**, 57 (1954).
10. Y. Merle, *J. Phys. Chem.,* **91**, 3093 (19878).
11. J. C. Salamone, L. Quach, A. C. Watterson, S. Krauser, and M. U. Mahmud, *J. Macromol. Scil, Part A,* **22**, 653 (1985).
12. D. N. Schulz, K. Kitano, J. A. Dannik, and J. J. Kaladas, *Polym. Mater. Sci. Eng.,* **147**, 149 (1987).
13. J. Corpart and F. Candau, *Macromolecules,* **26**, 1333 (1993).
14. J. C. Salamone, W. Volksen, S. C. Israel, A. P. Olson, and D. C. Raia, C., *Polymer,* **18**, 1058 (1977).
15. J. C. Salamone, W. Volksen, S. C. Israel, A. P. Olson, and D. C. Raia, C., *Polymer,* **19**, 1157 (1978).
16. V. M. Monroy Soto and J. C. Galin, *Polymer,* **25**, 121 (1984).
17. V. M. Monroy Soto and J. C. Galin, *Polymer,* **25**, 254 (1984).
18. D. N. Schulz, P. K. Peiffer, J. Agarwal, J. Larabee, J. J. Kaladas, L. Soni, B. Handwerker, and R. T. Garner, *Polymer,* **27**, 1734 (1986).
19. D. J. Liaw, W. F. Lee, Y. C. Whung, and M. C. Lin, *J. Appl. Polym. Sci.,* **34**, 999 (1987).
20. McCormick, C. L. and Salazar, L. C. *Polymer* 1992, **33**, 4617.

21. H. Ladenheim and H. Morawetz, *J. Polym. Sci.,* **26** (113), 251 (1957).

22. D. A. Topichiev, R. A. Mkrtchyan, R. A. Simonyan, and V. A. Kabanov, *Poym. Sci., USSR (Eng. Transl.)* ***A19***, 580 (1977).

23. (a) T. A. Wielema and J. B. F. N. Engberts, *Eur. Polymer J.* **24,** 647 (1988). (b) T. A. Wielema, *Ph.D. Dissertation*, University of Groningen, 1989.

24. M. Skouri, J. P. Munch, S. J. Candau, S. Neyret, and F. Candau, *Macromolecules,* **27**, 69 (1994).

25. D. G. Peiffer and R. D. Lundberg, *Polymer*, **26**, 1058 (1985).

26. J. C. Salmone, I. Ahmed, E. L. Rodriguez, L. Quach, and A. C. Watterson, *J. Macromol. Sci. Chem., Part A*, **25**, 811 (1988).

27. C. L. McCormick and C. B. Johnson, *Polymer*, **31**, 1100 (1990).

28. McCormick, C. L. and Salazar, L. C. *Polymer,* **33**, 4384 (1992).

29. C. L. McCormick and C. B. Johnson, *J. Macromol. Sci., Chem. Part A*, **27**, 539 (1990).

30. C. L. McCormick and L. C. Salazar, *J. Appl. Poly. Sci.*, **48**, 1115 (1993).

31. (a) E. E. Kathmann and C. L. McCormick, *Polym. Prepr. Am. Chem. Soc. Div. Polym. Chem.*, **35** (2), 641 (1994). (b) E. E. Kathmann, L. A. White, C. L. McCormick, *Polymer*, **38**, 879 (1997).

32. Kathmann, E. E.; Davis, D. D.; McCormick, C. L. *Macromolecules* **27**, 3156 (1994).

33. Laughlin, R. G. In *Advances in Liquid Crystals*, Vol. 3, Brown, G. H., Ed., Academic Press, New York, 1978, p. 41 and p. 99

34. Laughlin, R. G. *Langmuir*, **7**, 842 (1991).

35. P. Molyneux, *Water-Soluble Synthetic Polymers: Properties and Behavior, Vol. II,* CRC Press, Boca Raton, FL, 1984.

36. F. Ascoli and C. Botre, *J. Polym. Sci.* **62**, S56 (1962).

# CHAPTER 3. PH RESPONSIVE BEHAVIOR OF TERPOLYMERS OF SODIUM ACRYLATE, ACRYLAMIDE, AND THE ZWITTERIONIC MONOMER 4-(2-ACRYLAMIDO-2-METHYLPROPYLDIMETHYLAMMONIO)BUTANOATE: SOLUTION PROPERTIES

## INTRODUCTION

Our research efforts have been focused on the development of stimuli-responsive water-soluble polymers designed for use in oil field applications, particularly enhanced oil recovery (EOR). This chapter discloses the progress of our ongoing research of polybetaines, polymers derived from zwitterionic monomers, that show the ability to sustain or increase their solution viscosity in the presence of electrolytes.[1-6] Such polymers appear to be well-suited for use under conditions similar to those encountered in EOR operations.

In this investigation, the AADAB, AADAPS (terpolymers of NaA, AM, and 3-(2-acrylamido-2-methylpropyldimethylammonio)propanesulfonate (AMPDAPS)), and DABAM (copolymers of AM and AMPDAB) series are compared to determine the effects of the nature of the zwitterionic mer unit and the incorporation of NaA on solution behavior. Viscometric studies are performed to evaluate the effects of polymer concentration, added electrolytes, and solution pH on each polymer series.

## EXPERIMENTAL

### Viscosity Measurements

Polymer stock solutions were prepared by dissolving 0.6 g polymer in 300 mL deionized water ($C_p$ = 0.2 g/dL) a pH 8.5. For the electrolyte studies, the appropriate amount of salt was added after polymer dissolution in water to achieve the desired concentration. The solutions were then isoionically diluted to appropriate concentrations and allowed to age for 7 to 10 days before being analyzed with a Contraves LS-30 low shear rheometer. Adjustments to pH were accomplished by adding small aliquots of a concentrated HCl or NaOH solution via microsyringe. All solution viscosities were determined at 25 °C at a shear rate of 6 $s^{-1}$. Duplicate runs were conducted and reproducibility was found to be within ± 3-7%.

## RESULTS AND DISCUSSION

### Solution Behavior

The dissolution behavior of the AADAB terpolymers in preparing stock solutions (0.2 g/dL at pH 8.5) was found to be dependent on the polymer composition. For AADAB-5 and AADAB-40, complete dissolution was achieved in several days; however, AADAB-10 and AADAB-25 required 4 weeks. Although the latter two readily absorbed water, small, microgel-like particles necessitated longer dissolution times. Recently, we observed similar aggregation for copolymers of acrylamide with 60 and 75 mol% AMPDAB. The microgel-like particles

from those systems, however, were extremely persistent and could not be disrupted under a variety of conditions, including the addition of electrolytes, urea, and pH changes.[7]

In contrast to the carboxybetaine containing polymers, copolymers of acrylamide with the sulfobetaine monomer, AMPDAPS, yielded no visual evidence of microgel particles. However, viscosity studies suggested the presence of intermolecular associations in deionized water which could be disrupted by the addition of electrolytes.[8] The existence of intermolecular associations for low charge density polyampholytes has been reported.[7-14] Although the main driving force for the associative behavior of polyampholytes is due to coulombic attractions between the oppositely charged groups, the chemical structures of the individual mer units induce other interactions such as hydrogen bonding or hydrophobic effects which determine the overall solvation of the polymer in an aqueous medium.

**Effects of Polymer Concentration**

The effects of increasing polymer concentration on the apparent viscosities of the AADAB terpolymers are shown in Figure 3.1. The studies were conducted in deionized water at pH 8.5. Under these conditions, there is a charge imbalance associated with the terpolymers as a result of the ionized NaA mer units. Polyelectrolyte behavior is confirmed by the high solution viscosities at low polymer concentration. The magnitude of the viscosity is affected not only by molecular weight but also by charge density effects. For instance, AADAB-40, which has lower molecular weight than AADAB-5, exhibits much higher viscosity values due to the higher mol % of NaA incorporated into the terpolymer. The anionic groups of AADAB-40 are inherently closer to neighboring anionic sites resulting in a greater degree of chain extension.

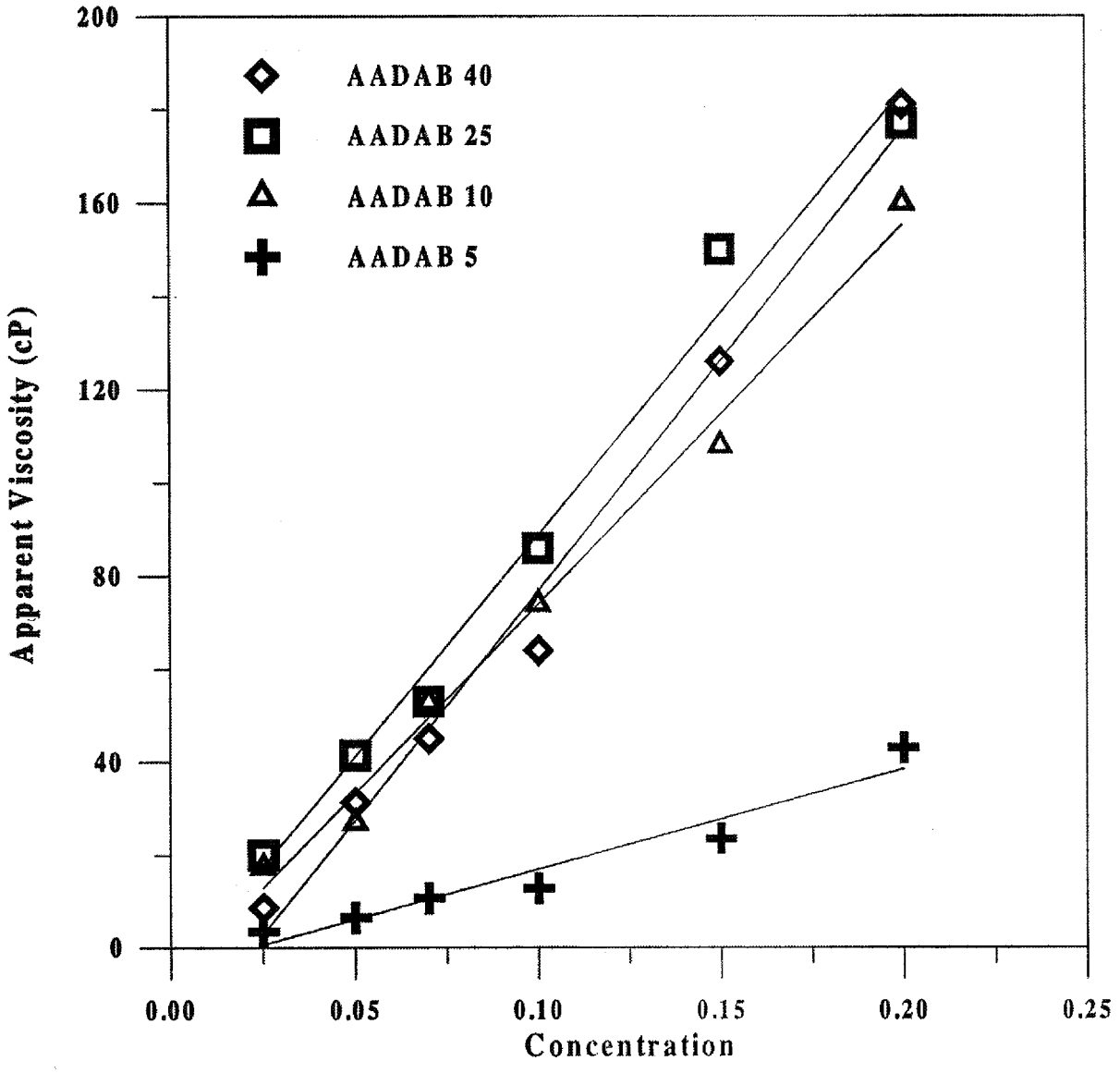


**Figure 3.1.** Apparent viscosity of AADAB terpolymers as a function of polymer concentration at pH 8.5.

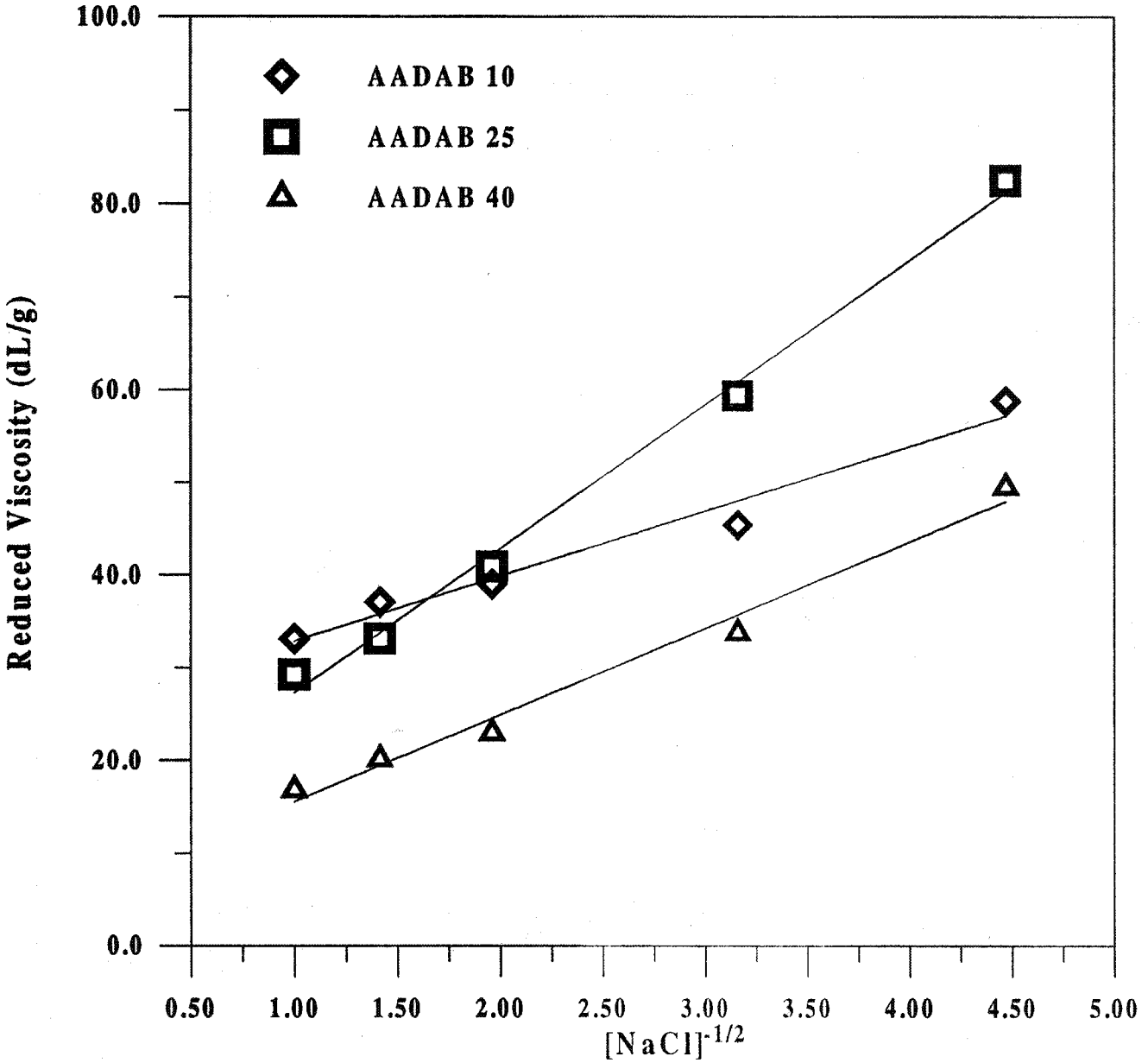


**Figure 3.2.** Reduced viscosity of AADAB terpolymers as a function of NaCl concentration at pH 8.5.

**Effects of Added Electrolytes**

A plot of the reduced viscosity versus $[NaCl]^{-1/2}$ for the AADAB terpolymers at pH 8.5 is presented in Figure 3.2. The linear behavior is typical of polyelectrolytes.[15] In the presence of added electrolytes, charge/charge repulsions between the anionic sites are shielded, leading to a decrease in the hydrodynamic volume as the polymer coil assumes a less extended conformation.

The magnitude of the slopes indicates the extent of conformational change induced by the addition of electrolytes. AADAB-10, with the lowest NaA incorporation, exhibits the smallest slope. AADAB-25 yields the highest slope, resulting from a combination of molecular weight and charge density effects. At higher concentrations of NaCl, AADAB-10 displays slightly higher viscosity values than AADAB-25 even though the molecular weight of AADAB-10 is substantially lower. This behavior is, in part, related to a decrease in the hydrophilicity of the polymer due to the higher incorporation of the AMPDAB mer unit. AADAB-40 has the lowest viscosity because the molecular weight is much lower than either AADAB-10 and AADAB-25 and electrolyte shielding allows conformational compaction.

**Effects of pH**

The reduced viscosity profiles of AADAB-10 and AADAB-40 as a function of decreasing pH were examined in deionized water and in 0.5 M NaCl; a representative profile is shown in Figure 3.3. In deionized water, both terpolymers exhibit a minimum in reduced viscosity between pH 4-4.5 as a result of undergoing a polyanion→polyzwitterion→polycation transition. As the pH of the medium is lowered by the addition of HCl, the NaA mer units become progressively protonated, thereby reducing the effects of charge-charge repulsions. Due to the zwitterionic nature of AMPDAB, the charge ratio between anionic and cationic groups approaches unity. Coulombic interactions between these groups lead to a reduction in the hydrodynamic volume and a minimum in the reduced viscosity is observed. Further lowering of the pH beyond this point results in protonation of the carboxylate groups of AMPDAB. As this progresses, the polymer acquires an overall cationic charge due to the remnant quaternary ammonium moieties on AMPDAB. Charge-charge repulsions of these groups cause an extension of the polymer coil. Viscosity response is similar to that of naturally occurring proteins and the synthetic copolymer of *N*,*N*-diethyallylamine and acrylic acid.[16] The minimum in viscosity occurs at the isoelectric point. The decrease in viscosity values at low pH (ca. 2) for the AADAB series is attributed to the increase in ionic strength of the medium due to the presence of hydronium and chloride ions as well as residual NaCl from the neutralization of the NaA mer units.

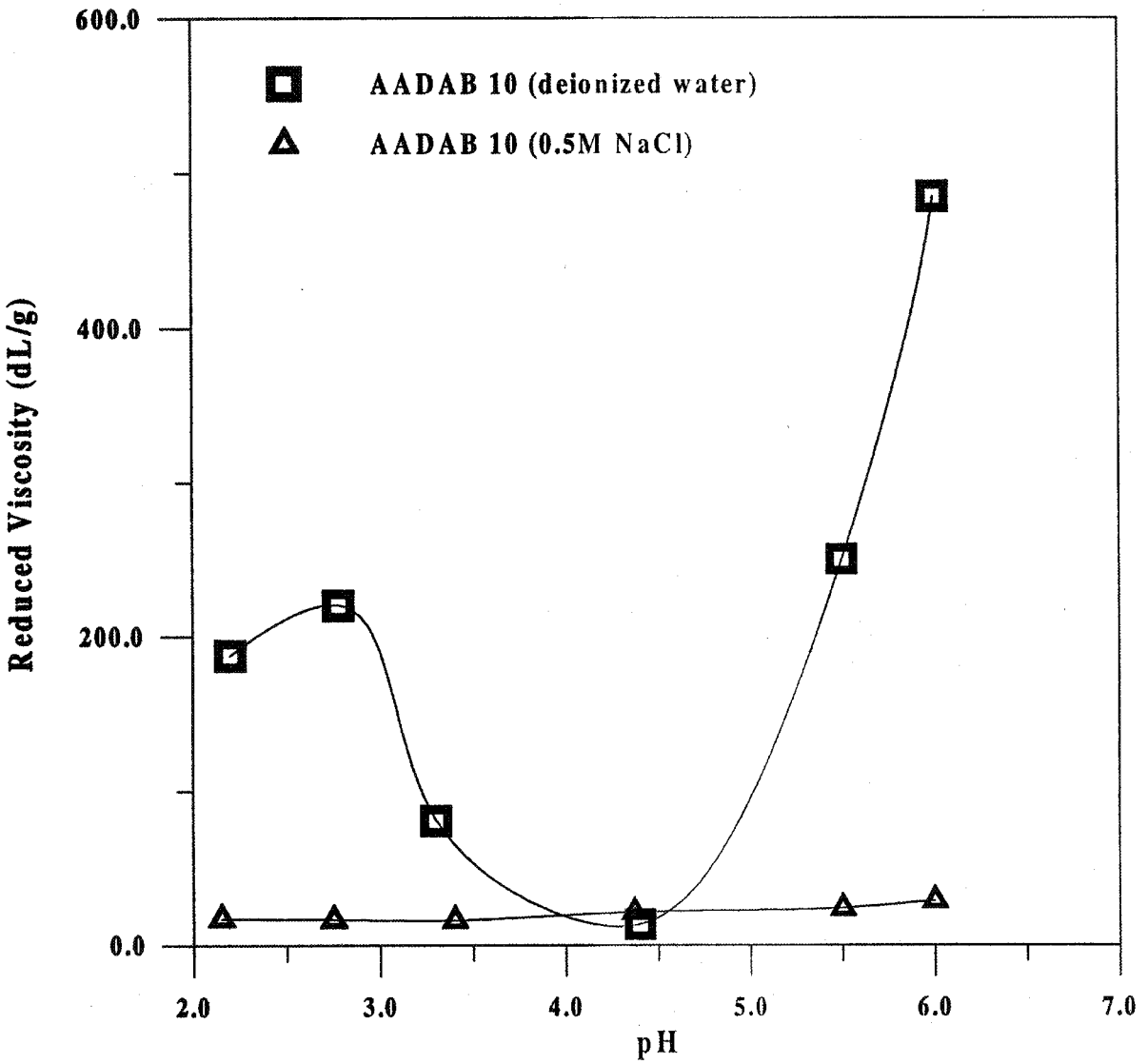


**Figure 3.3.** Reduced viscosity of AADAB-10 as a function of pH in deionized water and 0.5 M NaCl.

In 0.5 M NaCl, the minimum in viscosity is no longer observed as the repulsive forces between charges at high and low pH are shielded. In addition, AADAB-10 exhibits a higher reduced viscosity in 0.5 M NaCl than in deionized water (21.5 vs. 13.4 dL/g) at pH 4.4. AADAB-40 also exhibits this increase in viscosity; however, the differences are much smaller (7.1 vs. 6.4 g/dL). This enhancement is a result of the shielding of the attractive coulombic interactions as the charge ratio approaches unity, behavior typical of polyzwitterions.

It should also be noted that for AADAB-40 in 0.5 M NaCl, the reduced viscosity decreases from 18.0 to 4.0 dL/g as the pH value is lowered from pH 6.6 to pH 2.1. This behavior is likely a culmination of three effects. First, the strong interactions between water molecules and the carboxylate groups of the NaA mer unit are replaced by weaker interactions as

protonation to the carboxylic acid group occurs, thus reducing polymer solvation. Second, hydrogen bonding interactions between neighboring acrylamido and acrylic acid mer units results in a loss of the number of polymer sites available to interact with water molecules further reducing the polymer/solvent interaction. Third, in the presence of added electrolytes, which shield coulombic repulsions, an increase in the hydrophobicity of the polymer occurs as protonation of the butanoate moiety to butanoic acid (incorporated within the AMPDAB mer unit) progresses.

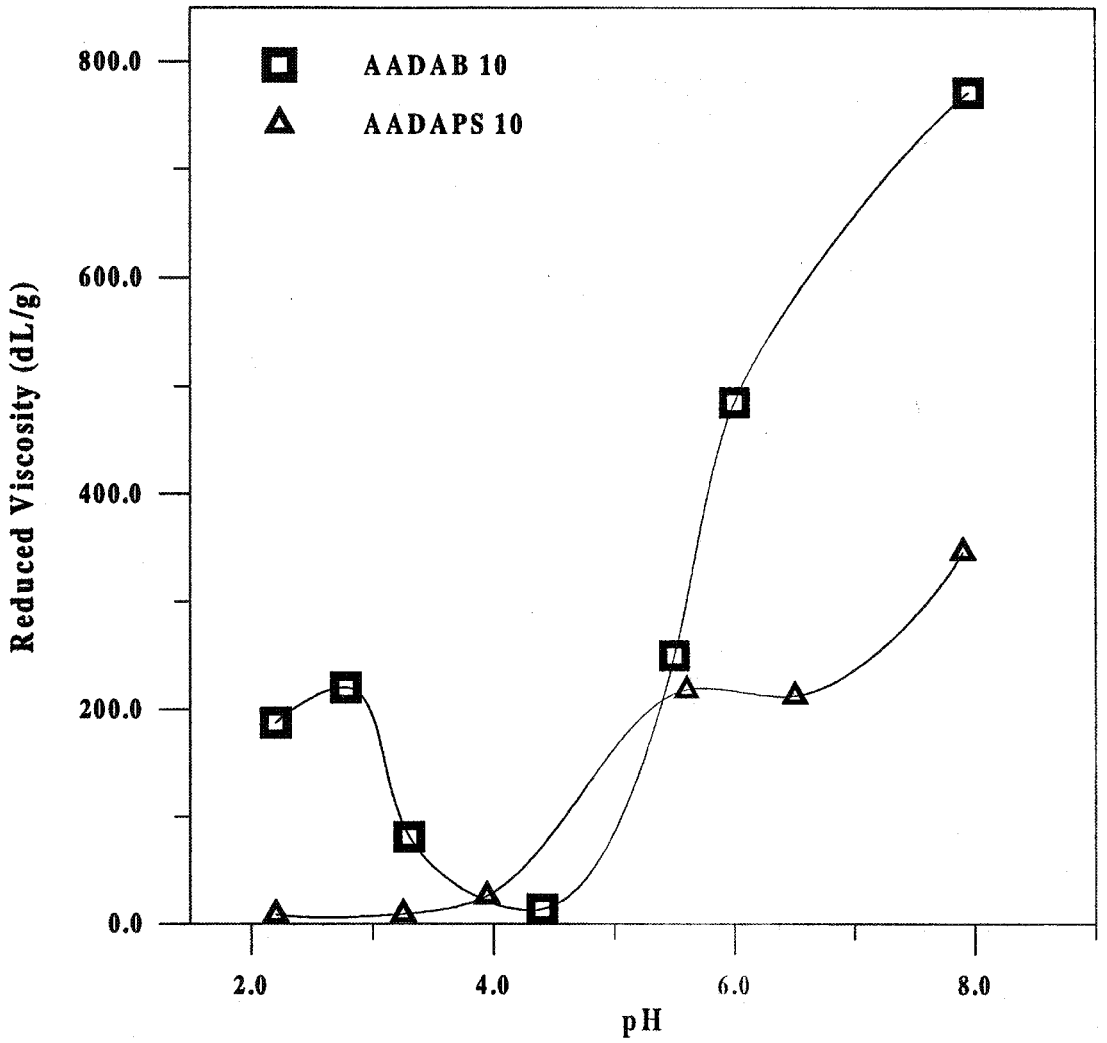


**Figure 3.4.** Reduced viscosity of AADAB-10 and AADAPS as a function of pH in deionized was ($C_p$ = 0.1 g/dL).

**Effects of the Nature of the Zwitterionic Mer Unit**

Shown in Figure 3.4 is the reduced viscosity as a function of pH for AADAB and AADAPS terpolymers at 10 mol % incorporation. The main distinction between the two terpolymers is the difference in basicity, the carboxylate group of AADAB being a stronger base than that of the sulfonate group of AADAPS. In aqueous solution, the carboxylate group can be

rendered nonionic by lowering pH; by contrast, the sulfonate group remains anionic even at low pH due to the inherently low $pK_a$ (< 0) of this group. Thus, for the AADAB terpolymers there is an enhancement in viscosity at low pH due to the polycationic nature. The AADAPS terpolymers do not exhibit this behavior because the sulfonate group is not protonated under these conditions and the terpolymers remain polyzwitterionic.

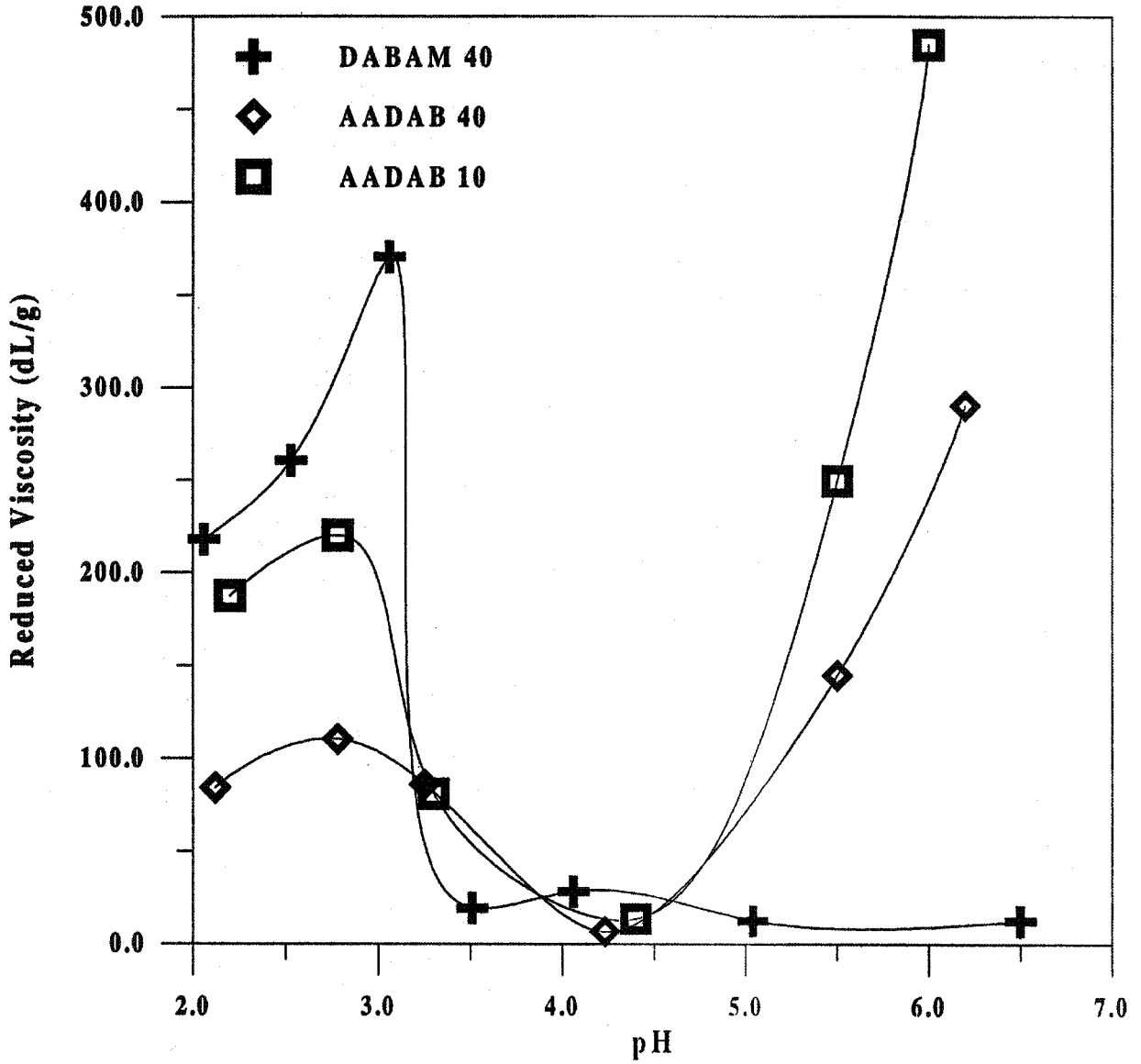


**Figure 3.5.** Reduced viscosity of AADAB-40, AADAB-10, and DABAM-40, as a function of pH in deionized water ($C_p$ = 0.1 g/dL).

**Effects of the Incorporation of NaA**

Figure 3.5 shows the reduced viscosity as a function of pH in deionized water for AADAB-10, AADAB-40, and DABAM-40. Both AADAB copolymers exhibit larger viscosities compared to DABAM-40 at higher pH values due to the presence of the NaA mer units. At low pH, all three polymers exhibit a maximum in viscosity as the polymers undergo the

polyzwitterion→polycation transition due to protonation of the AMPDAB mer units. Unfortunately, molecular weight differences preclude a meaningful structural comparison for AADAB-40 and DABAM-40 at low pH; however, it is likely that hydrogen bond formation between acrylic acid and acrylamide mer units in the AADAB terpolymer results in a lowering of the polymer/solvent interactions. AADAB-10 and DABAM-40 have similar molecular weights, but charge density differences also prevent direct comparisons.

## CONCLUSIONS

At pH 8.5, the AADAB terpolymers behave as polyelectrolytes due to the anionic charge provided by NaA mer units. High apparent viscosity values at low polymer concentration and the reduction of viscosity in the presence of small molecule electrolytes are evidence for polyanionic structure. The reduced viscosity of the AADAB terpolymers as a function of pH passes through a minimum as the terpolymer undergoes a polyanion→polyzwitterion→polycation transition upon lowering pH as a result of the protonation of the NaA and AMPDAB mer units. Terpolymers possessing sulfobetaine mer units, the AADAPS series, do not exhibit an enhancement in viscosity at low pH due to the weak basicity of the sulfonate group. In the presence of 0.5 M NaCl at pH 3, AADAPS-40 exhibits a higher viscosity than AADAB-40 resulting from increased hydrophobicity of the latter as the carboxybetaine mer units are protonated. AADAB-40 displays enhanced viscosity behavior at pH > 5 compared to DABAM-40 due to the ionization of the NaA mer units.

## REFERENCES


1. McCormick, C. L. and Johnson, C. B. *Macromolecules*, **21**, 687 (1988).
2. McCormick, C. L. and Johnson, C. B. *Macromolecules*, **21**, 694 (1988).
3. C. L. McCormick and L. C. Salazar, *Macromolecules* **25**, 1896 (1992).
4. T. Alfrey and H. Morawetz, *J. Am. Chem. Soc., 74*, **436** (1952).
5. T. Alfrey, R. Fuoss, H. Morawetz, and S. H. Pinner, *J. Am. Chem. Soc.,* **74**, 438 (1952).
6. T. Alfrey and S. H. Pinner, *J. Polym. Sci.,* **23**, 533 (1957).
7. D.O. Jordan and T. Kuruscev, *Polymer,* **1**, 185 (1960).
8. G. Ehrlich and P. Doty, *J. Am. Chem. Soc.,* **76**, 3764 (1954).
9. A. Katchalsky and I. R. Miller, *J. Polym. Sci.,* **13,** 57 (1954).
10. Y. Merle, *J. Phys. Chem.,* **91**, 3093 (19878).
11. J. C. Salamone, L. Quach, A. C. Watterson, S. Krauser, and M. U. Mahmud, *J. Macromol. Scil, Part A,* **22**, 653 (1985).
12. D. N. Schulz, K. Kitano, J. A. Dannik, and J. J. Kaladas, *Polym. Mater. Sci. Eng.,* **147**, 149 (1987).
13. J. Corpart and F. Candau, *Macromolecules,* **26**, 1333 (1993).
14. J. C. Salamone, W. Volksen, S. C. Israel, A. P. Olson, and D. C. Raia, C., *Polymer,* **18**, 1058 (1977).
15. J. C. Salamone, W. Volksen, S. C. Israel, A. P. Olson, and D. C. Raia, C., *Polymer,* **19**, 1157 (1978).
16. V. M. Monroy Soto and J. C. Galin, *Polymer,* **25**, 121 (1984).
17. V. M. Monroy Soto and J. C. Galin, *Polymer,* **25**, 254 (1984).
18. D. N. Schulz, P. K. Peiffer, J. Agarwal, J. Larabee, J. J. Kaladas, L. Soni, B. Handwerker, and R. T. Garner, *Polymer,* **27**, 1734 (1986).
19. D. J. Liaw, W. F. Lee, Y. C. Whung, and M. C. Lin, *J. Appl. Polym. Sci.,* **34**, 999 (1987).
20. McCormick, C. L. and Salazar, L. C. *Polymer* 1992, **33**, 4617.

21. H. Ladenheim and H. Morawetz, *J. Polym. Sci.,* **26** (113), 251 (1957).

22. D. A. Topichiev, R. A. Mkrtchyan, R. A. Simonyan, and V. A. Kabanov, *Poym. Sci., USSR (Eng. Transl.)* **A19**, 580 (1977).

23. (a) T. A. Wielema and J. B. F. N. Engberts, *Eur. Polymer J.* **24**, 647 (1988). (b) T. A. Wielema, *Ph.D. Dissertation*, University of Groningen, 1989.

24. M. Skouri, J. P. Munch, S. J. Candau, S. Neyret, and F. Candau, *Macromolecules,* **27**, 69 (1994).

25. D. G. Peiffer and R. D. Lundberg, *Polymer*, **26**, 1058 (1985).

26. J. C. Salmone, I. Ahmed, E. L. Rodriguez, L. Quach, and A. C. Watterson, *J. Macromol. Sci. Chem., Part A*, **25**, 811 (1988).

27. C. L. McCormick and C. B. Johnson, *Polymer*, **31**, 1100 (1990).

28. McCormick, C. L. and Salazar, L. C. *Polymer*, **33**, 4384 (1992).

29. C. L. McCormick and C. B. Johnson, *J. Macromol. Sci., Chem. Part A*, **27**, 539 (1990).

30. C. L. McCormick and L. C. Salazar, *J. Appl. Poly. Sci.*, **48**, 1115 (1993).

31. (a) E. E. Kathmann and C. L. McCormick, *Polym. Prepr. Am. Chem. Soc. Div. Polym. Chem.*, **35** (2), 641 (1994). (b) E. E. Kathmann, L. A. White, C. L. McCormick, *Polymer*, **38**, 879 (1997).

32. Kathmann, E. E.; Davis, D. D.; McCormick, C. L. *Macromolecules*, **27**, 3156 (1994).

33. Laughlin, R. G. In *Advances in Liquid Crystals*, Vol. 3, Brown, G. H., Ed., Academic Press, New York, 1978, p. 41 and p. 99

34. Laughlin, R. G. *Langmuir*, **7**, 842 (1991).

35. P. Molyneux, *Water-Soluble Synthetic Polymers: Properties and Behavior, Vol. II,* CRC Press, Boca Raton, FL, 1984.

36. F. Ascoli and C. Botre, *J. Polym. Sci.* **62**, S56 (1962).

# CHAPTER 4. ELECTROLYTE AND PH-RESPONSIVE ZWITTERIONIC COPOLYMERS OF 4-(2-ACRYLAMIDO-2-METHYLPROPYLDIMETHYL-AMMONIO) BUTANOATE WITH 3-(2-ACRYLAMIDO-2-METHYL-PROPYLDIMETHYLAMMONIO) PROPANESULFONATE: SYNTHESIS AND CHARACTERIZATION

## INTRODUCTION

Polyampholytes, unlike conventional polyelectrolytes, incorporate both anionically and cationically charged moieties into a single polymer chain. These systems exhibit unusual rheological behavior as a result of the attractive coulombic interactions between oppositely charged species. In addition, the solution behavior of polyampholytes is also related to the ratio of the ionic species incorporated into the polymer.[1-18] This ratio can be varied through synthetic methods as well as through extrinsic changes in the aqueous environment, particularly changes in pH. When an excess of either anionic or cationic groups is present, the systems behave as polyelectrolytes as typically evidenced by a viscosity decrease in the presence of small molecule electrolytes. However, as the ratio of anionic to cationic species approaches unity, the solution behavior is dominated by coulombic attractions. These attractions may, in many cases, render the polymer insoluble in deionized water, but soluble in the presence of a critical concentration of added electrolytes as the attractive charge/charge interactions are shielded. Higgs and Joanny have developed a theoretical treatment of the solution behavior of polyampholytes with varying charge ratios.[19] It was concluded that coulombic interactions, both attractive (polyampholyte contribution) and repulsive (polyelectrolyte contribution), dictate the solution behavior of these systems. Whether the polyampholyte or polyelectrolyte effect dominates the solubility of copolymers is dependent on both the charge ratio and concentration of small molecule electrolytes.

Zwitterionic monomers have been employed in the synthesis of polyampholytes.[20-42] These monomers are unique in that both the cationic and anionic charge are incorporated into the same mer unit and thus, at appropriate pH values, the resulting polyzwitterions will have a charge ratio of exactly one. The most thoroughly investigated polyzwitterions are based on sulfobetaine mer units in which the cationic moiety is a quaternary ammonium group and the anionic moiety a sulfonate group.[20-34] These polyzwitterions are typically insoluble in deionized water and require the addition of small molecule electrolytes to achieve solubility in aqueous media. Furthermore, the sulfonate group is a weak base and thus remains predominantly dissociated in aqueous media. Polyzwitterions based on carboxybetaine mer units in which the anionic species is a carboxylate group have also been investigated, although to a lesser degree.[37-42] These systems are usually more soluble in deionized water than the sulfobetaine analogs. In addition, these mer units can be converted from zwitterionic to cationic by lowering the pH, since the carboxylate groups (in contrast to sulfonate groups) can be protonated in aqueous media. Thus, for these systems, the charge ratio between anionic and cationic species can be varied by adjusting the pH.

The solution properties of polyampholytes based on the sulfobetaine monomer 3-(2-acrylamido-2-methylpropyldimethylammonio) propane sulfonate (AMPDAPS)[33] , **2**, and on the carboxybetaine analog 4-(2-acrylamido-2-methylpropyl dimethylammonio) butanoate (AMPDAB)[42] , **1**, have been elucidated previously in separate studies in our laboratories. It was found that the homopolymer of AMPDAPS, **C(0:100)**, was insoluble in deionized water at all pH values while the homopolymer of AMPDAB, **C(100:0)**, was soluble. Since the only structural variance between these two systems is the anionic group, the contrasting behavior must be attributed to solvation differences of the sulfonate and the carboxylate moieties of the zwitterionic group. To further investigate this behavior, we report in this paper the synthesis and characterization of a new series of copolymers of AMPDAB and AMPDAPS, **C(X:Y)**. The objective of this work is to compare the solution behavior of the two homopolymers of AMPDAB, **C(100:0)**, and AMPDAPS, **C(0:100)**, with copolymers, **C(X:Y)**, incorporating both zwitterionic monomers, **1** and **2**. It will be subsequently shown that conditions of pH, electrolyte concentration, and the nature of the anionic moiety incorporated into the zwitterionic mer unit dramatically affect the solubility and rheological behavior.

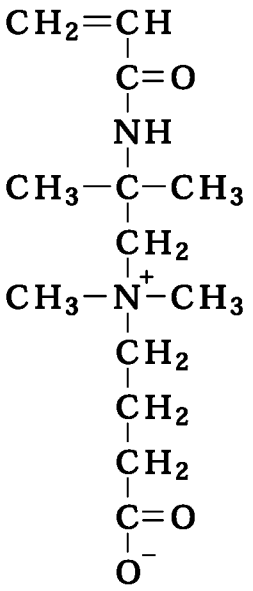

**1**

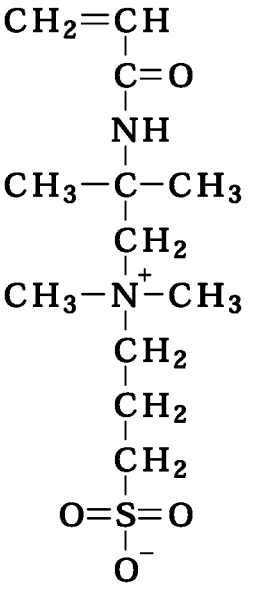

**2**

**Scheme 4.1.** 4-[(2-acrylamido-2-methylpropyldimethylammonio)]butanoate (AMPDAB, 1), and 3-[(2-acrylamido-2-methylpropyldimethylammonio)]propanesulfonate (AMPDAPS, 2).

## EXPERIMENTAL

### Materials and Methods

4-(2-acrylamido-2-methylpropanedimethyl ammonio)butanoate (AMPDAB) was synthesized by the quaternization reaction of 2-acrylamido-2-methylpropanedimethyl amine with ethyl 4-bromobutyrate followed by hydrolysis of the ester functionality as previously reported.[7]

The synthesis of 3-(2-acrylamido-2-methylpropyldimethylammonio) propanesulfonate (AMPDAPS), has been reported previously.[7] Briefly, AMPDAPS was synthesized by the ring

opening reaction of 1,3-cyclopropane sultone with acrylamido-2-methylpropanedimethylamine in the presence of acetone at 45°C. The product precipitated from the reaction medium and was subsequently washed with acetone and ether to yield pure AMPDAPS. The product was then recrystallized from ethanol.

Potassium persulfate from J. T. Baker was recrystallized twice from deionized water. All other materials were used as received.

$^{13}C$ NMR spectra of the copolymers were obtained at 50.3 MHz with a Bruker AC200 spectrometer using 15-20 wt % 0.5 M NaCl ($D_2O$) polymer solutions with DSS (3-(trimethylsilyl)-1-propane-sulfonic acid, sodium salt) as a reference. A recycle delay of 8 s, 90° pulse length, and inverse gated decoupling to remove the Nuclear Overhauser Effect (NOE) were used for quantitative spectral analysis. Compositions were determined by integration of the geminal dimethyl resonances of each monomer. These data are accurate within $\pm$ 5 mol%.

Molecular weight studies were performed with a Chromatix KMX-6 low angle laser light scattering instrument at 25 °C in 1.0M NaCl. Refractive index increments were obtained using a Chromatix KMX-16 laser differential refractometer.

**Synthesis of Copolymers of 4-(2-acrylamido-2-methylpropanedimethyl ammonio)-butanoate, with 3-(2-Acrylamido-2-Methylpropyldimethyl ammonio) Propanesulfonate**

The homopolymers of AMPDAB and AMPDAPS, as well as the copolymers of AMPDAB with AMPDAPS, were synthesized by free radical polymerization in a 0.5 M aqueous NaBr solution under nitrogen at 30°C using 0.1 mol % potassium persulfate as the initiator. The feed ratio of AMPDAB:AMPDAPS was varied from 100:0 to 0:100 mol % with the total monomer concentration held constant at 0.45 M. NaBr was added to insure that the polymerization medium remained homogeneous.

In a typical synthesis, specified quantities of each monomer were dissolved in small volumes of deionized water. The separate solutions were then combined and one equivalent of sodium hydroxide per equivalent of AMPDAB was added and the pH adjusted to 8. The necessary quantity of NaBr was then added to achieve a 0.5 M NaBr solution. The reaction mixture was sparged with nitrogen and initiated with 0.1 mol % potassium persulfate. The reaction was terminated around 40-60% conversion due to the high viscosity of the reaction medium. The polymers were precipitated in acetone, dissolved in deionized water, then dialyzed against deionized water adjusted to pH=8.5 using Spectra/Por 4 dialysis bags with molecular weight cutoffs of 12,000 to 14,000 g/mol. The homopolymer of AMPDAPS precipitated from solution during dialysis. The polymers were isolated by lyophillization and conversions were determined gravimetrically from the purified polymers.

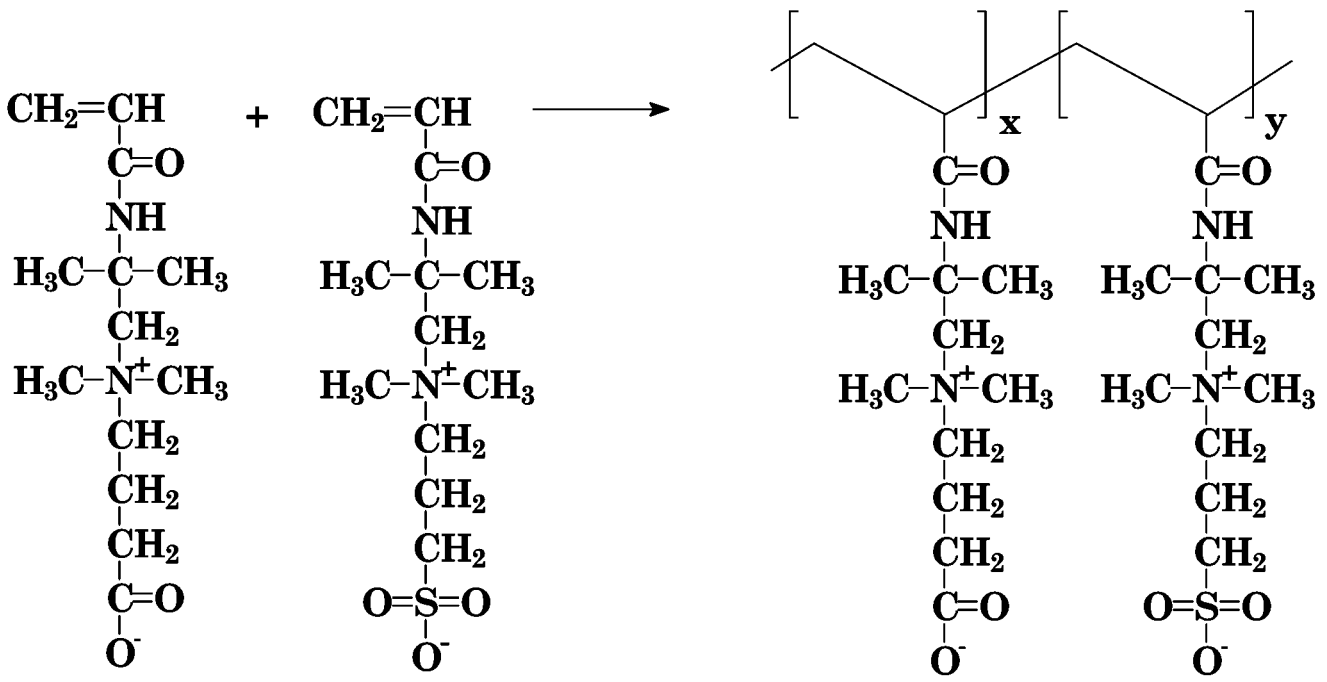

**Scheme 4.2.** Structural composition of copolymers of 4-(2-acrylamido-2-methylpropyldimethylammonio) Butanoate with 3-(2-acrylamido-2-methyl propyldimethylammonio) Propanesulfonate.

## RESULTS AND DISCUSSION

### Compositional Analysis

Copolymers were synthesized by varying the feed ratios of AMPDAB and AMPDAPS over the entire compositional range. Copolymer compositions were determined from $^{13}C$ NMR analysis by integration of the geminal dimethyl carbon resonances of the respective comonomers. Reaction parameters of feed ratios, reaction time, conversion, and composition are given in Table 4.1. Random copolymerization under the experimental conditions is expected due to similarity of the monomers. Compositions of the copolymers are designated **C(X:Y)** where X and Y represent the relative mole percent of AMPDAB, and AMPDAPS, respectively in the copolymer.

**Table 4.1. Reaction Parameters for the Copolymerization of 4-(2-Acrylamido-2-Methylpropyldimethylammonio) Butanoate (AMPDAB) with 3-(2-Acrylamido-2-Methylpropyldimethylammonio) Propanesulfonate (AMPDAPS).**

| Sample | Feed ratio (mol%) ( AMPDAB : AMPDAPS ) | Rxn. Time (hr.) | % Conv. | AMPDAB Found[a] (mol %) |
|---|---|---|---|---|
| C(0:100) | 0.0 : 100.0 | 3.0 | 60 | 0.0[b] |
| C(25:75) | 25.0 : 75.0 | 4.0 | 45 | 25 ± 5 |
| C(50:50) | 50.0 : 50.0 | 4.0 | 43 | 50 ± 5 |
| C(75:25) | 75.0 : 25.0 | 4.0 | 41 | 75 ± 5 |
| C(100:0) | 100.0 : 0.0 | 4.0 | 52 | 100.0[b] |

[a]Determined from $^{13}C$ N.M.R.

[b]Theoretical Value

**Low-Angle Laser Light Scattering**

Apparent weight average molecular weights as determined by low angle laser light scattering at 25 °C in 1.0M NaCl (Table 2) vary from 1.65 X $10^6$ to 3.95 X $10^6$ g/mol. The homopolymer of AMPDAPS, **C(0:100)** and the copolymers **C(25:75)** and **C(50:50)** have similar degrees of polymerization while **C(75:25)** has the lowest. The second virial coefficients ($A_2$) were also determined and range from 0.8 X $10^{-4}$ to 3.9 X $10^{-4}$ ml mol/$g^2$. In general, it is observed that the lower the molecular weight, the higher the $A_2$ value for a given polymer.

**Table 4.2. Classical Light Scattering Data for the Copolymers of4-(2-Acrylamido-2-Methylpropyldimethylammonio) Butanoate (AMPDAB) with 3-(2-Acrylamido-2-Methylpropyldimethylammonio) Propanesulfonate (AMPDAPS).**

| Sample | (AMPDAB) found[a] (mol %) | $M_W$ x $10^{-6}$ (g / mol) | $A_2$ x $10^4$ (ml·mol/$g^2$) | DP x $10^{-4}$ |
|---|---|---|---|---|
| C(0:100) | 0.0[b] | 3.1 | 1.2 | 1.1 |
| C(25:75) | 25.0 | 2.95 | 1.2 | 1.0 |
| C(50:50) | 50.0 | 2.36 | 2.7 | 0.9 |
| C(75:25) | 75.0 | 1.65 | 3.9 | 0.6 |
| C(100:0) | 100[b] | 3.9 | 0.8 | 1.5 |

[a]Determined from $^{13}C$ N.M.R.
[b]Theoretical Value

## CONCLUSION

The carboxybetaine monomer AMPDAB has been successfully copolymerized with the sulfobetaine monomer AMPDAPS by free radical polymerization in 0.5 M aqueous NaBr solution using potassium persulfate as the initiator. Copolymer compositional studies by $^{13}C$ NMR indicate that the monomer incorporation ratio is essentially the same as the feed ratio. Molecular weights range from 1.65 to 3.9 $\times$ $10^6$ g/mol, as determined by low-angle laser light scattering. In ongoing work, the AMPDAB:AMPDAPS copolymer series will be compared to determine the effects of the nature of the zwitterionic mer unit on solution behavior. Solubility, viscosimetric, and turbidimetric studies will be performed to evaluate the effects of polymer concentration, added electrolytes, and solution pH on each polymer series.

## REFERENCES


1. McCormick, C. L.; Johnson, C. B. *Macromolecules*, **21**, 687 (1988).

2. McCormick, C. L.; Johnson, C. B. *Macromolecules*, **21**, 694 (1988).

3. McCormick, C. L.; Salazar, L. C. *Polymer*, **33**, 4384 (1992).

4. McCormick, C. L.; Salazar, L. C. *Polymer,* **33**, 4617 (1992).

5. McCormick, C. L.; Salazar, L. C. *Macromolecules*, **25**, 1896 (1992).

6. McCormick, C. L.; Salazar, L. C. *J. Appl. Poly. Sci.*, **48**, 1115 (1993).

7. Salamone, J. C.; Volksen, W.; Israel, S. C.; Olson, A. P.; Raia, D. C.; *Polymer*, **18**, 1058 (1977).

8. Monroy Soto, V. M.; Galin, J. C. *Polymer*, **25**, 121 (1984).

9. Monroy Soto, V. M.; Galin, J. C. *Polymer*, **25**, 254 (1984).

10. Higgs, P. G. and Joanny, J. F., *J. Chem. Phys.*, **94**, 1543 (1991).

11. Schulz, D. N.; Peiffer, P. K.; Agarwal, J.; Larabee, J.; Kaladas, J. J.; Soni, L.; Handwerker, B.; Garner, R. T. *Polymer*, **27**, 1734 (1986).

12. Salamone, J. C.; Quach, L.; Watterson, A. C.; Krauser, S.; and Mahmud M. U. *J. Macromol. Sci., Part A*, *22*, 653 (1985).

13. Corpart, J.; Candau, F. *Macromolecules* , **26**, 1333 (1993).

14. Skouri, M.; Munch, J. P.; Candau, S. J.; Neyret, S.; Candau, F. *Macromolecules* , **27**, 69 (1994).

15. Peiffer, D. G.; Lundberg, R. D. *Polymer*, **26,** 1058 (1985).

16. Liaw, D. J.; Lee, W. F. ; Whung, Y. C.; Lin, M. C. *J. Appl. Polym. Sci.*, **37**, 999 (1987).

17. Salamone, J. C.; Volksen, W.; Israel, S. C.; Olson, A. P. *Polymer*, **19**, 1157 (1978).

18. Schulz, D. N.; Kitano, K.; Dannik, J. A.; Kaladas, J. J. *Polym. Mater. Sci. Eng.*, **147**, 149 (1987).

19. Ladenheim, H.; Morawetz, H. *J. Polym. Sci.,* **26***(113)*, 251 (1957).

20. Topichiev, D. A.; Mkrtchyan, R. A.; Simonyan, R. A.; Kabanov, V. A. *Polym. Sci., U.S.S.R. (Eng. Transl.)*, **A19**, 580 (1977).

21. Wielma, T., *PhD Dissertation*, University of Groningen, 1989.

22. Laughlin, R.G. *U.S. Patent 4,287,174*, **1981**.

23. Chevalier, Y.; Storet, Y.; Pourchet, S.; LePerchec, P. *Langmuir,* **7**, 848 (1991).

24. Weers, J. G.; Rathman, J. F.; Axe, F. U.; Crichlow, C. A.; Foland, L.D.; Scheuing, D. R.; Wiersema, R.J.; Zielske, A. G. *Langmuir,* **7**, 854 (1997).

25. McCormick, C.L.;Salazar, L.C *J. Polym. Sci., Part A*, **31**, 1099 (1993).

26. McCormick, C.L.;Blackmon, K.P. *Polymer,* **27**, 1971 (1986).

27. Fineman, M.; Ross, S. *J. Polym. Sci.*, **5**, 259 (1950).

28. Kelen, T.; Tudos, F. *J. Macromol. Sci., Chem.,* **A9**, 1 (1975).

29. Tidwell, P. W.; Mortimer, G. A. *J.Polym. Sci.:Part A*, **3**, 369 (1965).

30. Igarashi, S. *J. Polym. Sci., Polym. Lett. Ed.*, **1**, 359 (1963).

31. Salamone, J. C.; Ahmed, I.; Rodriguez, E. L.; Quach, L.; Watterson, A. C. *J. Macromol. Sci. Chem., Part A*, **25**, 811 (1988).

32. Laughlin, R.G. In *Advances in Liqid Crystals*; Brown G.H.,Ed.; Academic Press: New York, **1978**; *Vol. 3*, p41 and p99.

33. Collins, K.D.; Washabaugh, M. W. *Quat. Rev. of Biophys.*, **18(4)**, 323 (1985).

34. Molyneux, P. Water-Soluble Synthetic Polymers: Properties and Behavior, Vol. II; CRC Press: Boca Raton, FL., 1984.

35. Yasuzawa, M., Nakaya, T., and Imoto, M., *J. Macromol. Sci. Chem. Part A*, **23(8)**, 963 (1986).

36. Pujol-Fortin, M. L. and Galin, J. C., *Polymer,* **35**, 1462 (1994).

37. Ladenheim, H. and Morawetz, *J. Polym. Sci.*, **26**, 251 (1957).

38. Rosenheck, K. and Katchalsky, A, *J. Polym. Sci.*, **32**, 511 (1958).

39. Topchiev, D. A., Mkrtchyan, L. A., Simonyan, R. A., Lachinov, M. B., and Kabanov, R. A., *Polym. Sci. U.S.S.R. (Eng. Transl.)* **A19**,580 (1977).

40. (a)Wielema, T. A. and Engberts, J. B. F. N., *Eur. Polymer J.,* 1**988**, *24*, 647. (b) Wielma, T.A. PhD Dissertation, University of Groningen, 1989.

41. Hsu, Y. G., Hsu, M. J., Chen, K. M., *Makromol. Chem.*, **192**, 999 (1991).

42. (a) Kathmann, E. E. and McCormick, C. L., *Polym. Prepr. Am. Chem. Soc. Div. Polym. Chem.* **35(2)**, 641 (1994). (b) Kathmann, E. E., White, L. A., McCormick, C. L., *Polymer,* **38(4)**, 879-886 (1997).

43. McCormick, C.L.;Salazar *J. Polym. Sci., Part A*, **31**, 1099 (1993).

44. McCormick, C.L.;Blackmon, K.P. *Polymer,* **27**, 1971 (1986).

45. Collins, K.D.; Washabaugh, M. W. *Quat. Rev. of Biophys.*, **18(4)**, 323 (1985).

46. Laughlin, R.G. In *Advances in Liqid Crystals*; Brown G.H.,Ed.; Academic Press: New York, 1979, Vol 3, p.41 and 99

47. McCormick, C. L.; Elliott, D. L. *Macromolecules,* **19**, 687 (1986).

48. McCormick, C. L.; Newman, J. K. *Macromolecules,* **27**, 5114 (1994).

49. Stejskal, J.; Benes, M. I.; Kratochvil, P. *J. Polym. Sci., Polym. Phys. Ed.*, **12**, 1941 (1974).

# CHAPTER 5. ELECTROLYTE AND PH-RESPONSIVE ZWITTERIONIC COPOLYMERS OF 4-(2-ACRYLAMIDO-2-METHYLPROPYLDIMETHYL-AMMONIO) BUTANOATE WITH 3-(2-ACRYLAMIDO-2-METHYLPROPYL-DIMETHYLAMMONIO) PROPANESULFONATE: SOLUBILITY STUDIES

## INTRODUCTION

Our research efforts have been focused on the development of stimuli-responsive water-soluble polymers designed for use in enhanced oil recovery (EOR) applications. These model systems are tailored for potential application as viscosifiers and/or mobility control agents for secondary and tertiary EOR methods. The following report discloses the progress of our ongoing research of polybetaines, polymers derived from zwitterionic monomers, that show the ability to sustain or increase their hydrodynamic volume (and thus, solution viscosity) in the presence of electrolytes.[1-6] Such polymers appear to be well suited for use under conditions similar to those encountered in EOR operations.

Previoulsy, we have described the synthesis and characterization of amphoteric copolymers of the carboxybetaine monomer 4-[(2-acrylamido-2-methylpropyldimethylammonio)]butanoate (AMPDAB), with the sulfobetaine monomer 3-[(2-acrylamido-2-methylpropyldimethylammonio)]propanesulfonate (AMPDAPS). In this most recent investigation, the solution behavior of this copolymer series is studied using turbidimetric techniques. It is shown that conditions of pH, electrolyte concentration, and the nature of the anionic moiety incorporated into the zwitterionic mer unit dramatically affect the solubility behavior.

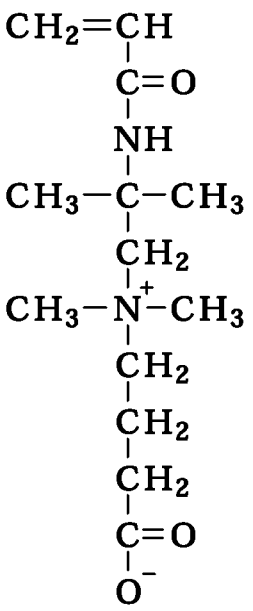

1

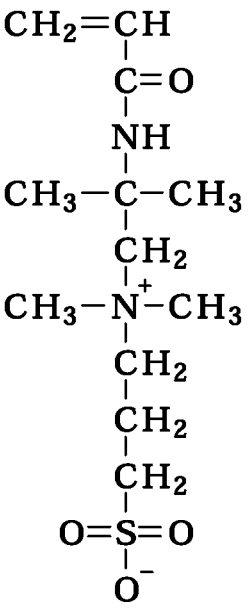

2

**Scheme 5.1.** 4-[(2-acrylamido-2-methylpropyldimethylammonio)]butanoate (AMPDAB, 1), and 3-[(2-acrylamido-2-methylpropyldimethylammonio)]propanesulfonate (AMPDAPS, 2).

## EXPERIMENTAL

### Turbidimetry

Polymer solutions were made by dissolving designated amounts of polymer in the stock electrolyte solutions. The solutions were then isoionically diluted to appropriate concentrations and allowed to age for 7-10 days prior to analysis. Phase separation was monitored using a Brinkman PC 800 Colorimeter using a 620 nm light filter. The sample of polymer solution (15 mL) was stirred by a magnetic stirrer and small aliquots of a concentrated HCl or NaOH solution were added by a microsyringe An electrode immersed in the solution was used to determine the pH value at which the phase transition occurred. Values were recorded when the transmittance was approximately 50%. The measurements were performed at least twice and were reproducible to within $\pm$ 0.2 of the listed pH values at 25$^{o}$C. The transitions were found to be sensitive to changes in the solution temperature.

## RESULTS AND DISCUSSION

### Behavior in Aqueous Solution

The behavior of the copolymer series in aqueous media is best analyzed by considering the expected charge distribution (Scheme 5.2) of the mer units of the copolymers as well as the homopolymers of AMPDAB, **1**, and AMPDAPS, **2**. The sulfonate moiety, a weak conjugate base, will remain in the dissociated, anionic form at all but the extremely low pH values (<0). In contrast, the carboxylate anion, a stronger conjugate base, can be protonated and thus rendered electrically neutral as pH values approach 4. This, of course, assumes complete hydration with no hydrophobic or electrostatic effects from neighboring groups.

In the copolymers of **1** and **2**, we can expect to encounter complex solution behavior based on ion pairing of the zwitterionic species on both the sulfobetaine and carboxybetaine mer units and preferential solvation dependent on composition and ionic character of the repeating units under specific conditions of pH and added electrolyte. Additionally we must consider repulsive and attractive coulombic interactions, counterion condensation, and hydrophobic effects.

In order to systematically examine solution behavior, it is first necessary to consider the nature of the repeating units in the **C(X:Y)** copolymers. Scheme 2 presents a simplistic picture of the expected charge distribution at: a) low, b) intermediate, and c) high pH. Of course, coulombic interactions change dramatically with ionic strength and are greatly affected by local dielectric constant.

The discussion to follow considers solubility (phase behavior) at 25$^{o}$C for the homopolymers and selected copolymers under selected conditions of pH, ionic strength, and added electrolyte type. Two polymer concentrations were chosen (0.2 and 0.5 g/dL) for these studies.

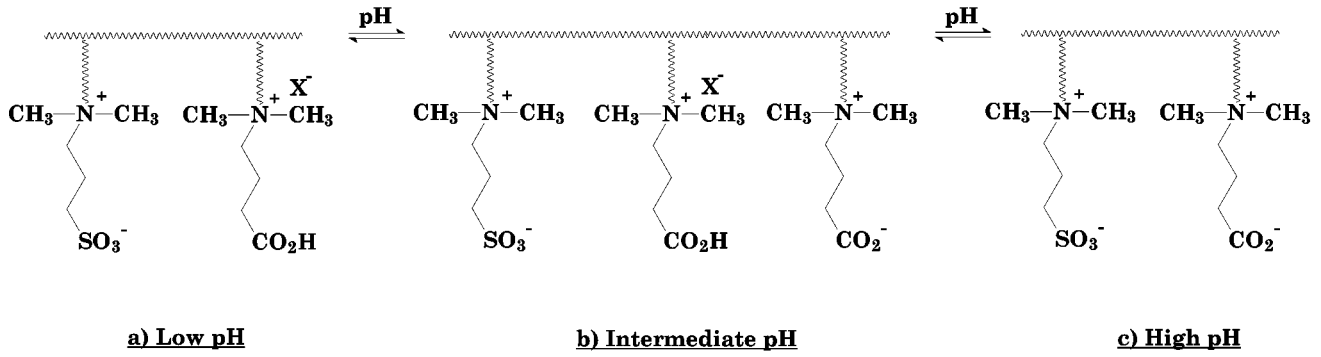


**Scheme 5.2.** Expected Charge Distribution in C(X:Y) Copolymers at Values of (a) Low, (b), Intermediate, and (c) High pH.

**Solubility Behavior**

**C(0:100)**, the homopolymer of **1**, is insoluble in deionized water at all pH values investigated in this study (pH=1-13). This behavior is typical of polyzwitterions composed of sulfobetaines with three methylene units between the cationic and anionic groups; the lack of solubility is attributed to the attractive coulombic interactions. These interactions, however, can be shielded by the addition of electrolytes resulting in solubilization of the polymer. The concentration of electrolyte required for dissolution is dependent on the nature of the electrolyte. Table 1 lists the critical electrolyte concentration (C.E.C.) required for solubilization of **C(0:100)** by various electrolytes. The "salting in" ability of the various electrolytes is in accord with the Hoffmiester series for the anions,[7] $SCN^- > Br^- > Cl^-$; similar rankings have been previously observed for poly(sulfobetaines).[8-11] This behavior has been rationalized in terms of "hard-soft" acid-base interactions. "Soft" (larger, more highly polarizable) anions are better adapted to interact with the "soft" quaternary ammonium group. This enhanced interaction results in a lower concentration of added electrolytes required to disrupt the attractive coulombic interactions of the poly(sulfobetaine) and, therefore, more efficiently facilitates solubilization of the polymer. Water structuring effects may also be operative.

**Table 5.1. Critical Electrolyte Concentration (CEC) Required for Solubilization of C(0:100)**

| Salt | CEC (M) |
|---|---|
| NaCl | 0.17 |
| CsCl | 0.2 |
| NaBr | 0.06 |
| NaSCN | 0.02 |

Interestingly, **C(100:0)**, the homopolymer of the carboxybetaine mer unit, is soluble in deionized water at all pH values up to 13, the highest value investigated in this study. The solubility of **C(100:0)** and the insolubility of **C(0:100)** in deionized water cannot be explained solely by charge balance since both mer units are zwitterionic at high pH values. It follows that differences in zwitterion solvation must be due to the anionic moieties. The differences in the solubility support the findings of Laughlin, who reported that surfactants possessing a carboxybetaine head group are more hydrophilic than those possessing a sulfobetaine head group based on phase behavior, basicity, and chromatographic data.[12] The enhanced hydration of the carboxylate group compared to that of the sulfonate group weakens the coulombic interaction with the ammonium group and, therefore, imparts solubility to **C(100:0)** in deionized water.

In deionized water, **C(25:75)** (possessing 25 mol% carboxybetaine and 75 mol% sulfobetaine) is soluble at pH values less than 8. At pH $\leq$ 8, sufficient numbers of the carboxylate groups of AMPDAB are protonated such that the polymer coil acquires a net positive charge. Solubilization of the polymer results when charge-charge repulsions between the cationic groups reaches a critical limit. Conversely, above pH 8, charge repulsions are diminished as **1** is rendered zwitterionic and the charge ratio approaches unity. The attractive coulombic interactions between the anionic and cationic charge centers result in phase separation. Copolymers **C(50:50)** and **C(75:25)** and homopolymer **C(100:0)** do not display this behavior and are soluble in deionized water throughout the pH range investigated (pH 1-13). The insolubility of **C(25:75)** at pH $\geq$ 8 is, therefore, likely a result of the higher incorporation of the sulfobetaine mer unit in the copolymer, a conclusion supported by the insolubility of **C(0:100)** in deionized water. Accordingly, the solubility of **C(50:50)** and **C(75:25)** can be attributed to the higher incorporation of the carboxybetaine mer units into these copolymers.

The solubility behavior of **C(25:75)** as a function of pH and polymer concentration in the presence of added electrolytes is presented in Table 5.2. As will be discussed below, complex behavior is observed and explained in terms of competitive interactions affecting solubility. A consideration of the ionization state (ionic or zwitterionic), Scheme 5.2, and the effect of electrolyte on the degree of chain solvation (contraction or expansion) is essential. For example, in the presence of 0.008 M NaCl ($C_p$=0.2 g/dL), lower pH values (7.6 vs. 8) are necessary for solubilization of **C(25:75)** as compared to deionized water. The presence of NaCl slightly shields the initial charge repulsions thus requiring that more of the carboxybetaines units be rendered cationic for subsequent solubilization. At pH $\geq$ 7.6, charge/charge interactions between the anionic and cationic groups result in phase separation. Apparently, 0.008 M NaCl is not a sufficient concentration of electrolyte to shield the shorter range attractive interactions.

**Table 5.2. Phase Behavior of C(25:75) as a Function of pH[a]**

| Salt Concentration (M) | 0.02 g/dL | | | | 0.05 g/dL | | | |
|---|---|---|---|---|---|---|---|---|
| | NaCl | CsCl | NaBr | NaSCN | NaCl | CsCl | NaBr | NaSCN |
| 0.008 | $7.6^{ia}$ | - | - | - | - | - | - | - |
| 0.017 | $9.6^{ib}$<br>$4.6^{ia}$ | - | - | - | $9.4^{ib}$<br>$4.4^{ia}$ | - | - | - |
| 0.05 | $8.6^{ib}$ | $8.2^{ib}$ | $6.0^{ib}$ | $4.6^{ib}$ | $8.9^{ib}$ | $8.7^{ib}$ | $8.3^{ib}$ | $7.0^{ib}$ |
| 0.1 | $6.0^{ib}$ | $5.8^{ib}$ | $4.2^{ib}$ | $3.7^{ib}$ | $8.2^{ib}$ | $8.0^{ib}$ | $7.3^{ib}$ | $4.0^{ib}$ |
| 0.3 | $3.9^{ib}$ | $3.8^{ib}$ | - | - | $4.4^{ib}$ | $4.1^{ib}$ | - | - |
| 0.5 | - | - | - | - | - | - | - | - |

[a] ib = insoluble below listed pH. ia = insoluble above listed pH. - = no phase separation observed between pH 1 and 13

As the concentration of NaCl is increased (0.017 M NaCl), a region of insolubility between pH 9.6 and 4.6 occurs. In this intermediate pH region, **C(25:75)** can be considered to be a terpolymer of sulfobetaine mer units, carboxybetaine mer units, and quaternary ammonium mer units (Scheme 2b). The resulting insolubility is likely due to two factors. First, as the carboxybetaine mer units become protonated, the hydrophobicity of the copolymer increases due to the loss of the anionic charge center which was previously hydrated. Second, **C(25:75)** is composed of 75 mol% sulfobetaine moieties; functional groups which , when incorporated into polymers, typically require the addition of a critical concentration of electrolyte to facilitate solubilization. Above pH 9.6, **C(25:75)** is essentially polyzwitterionic and the presence of NaCl aids the solubilization by shielding the attractive coulombic interactions (Scheme 5.2c). Below this pH, the carboxybetaine groups become protonated; however, the higher concentration of NaCl (0.017 M vs. 0.008 M) efficiently shields the initial cationic sites and thus prevents solubilization. As the pH approaches 4.6, however, a sufficient number of the carboxybetaine groups are rendered cationic such that the repulsions are no longer shielded; i.e. spatial distance is likely approaching the Debye-Huckel reciprocal screening length. As this occurs, solubility is achieved due to coulombic repulsions (Scheme 2a).

When the NaCl concentration is further increased to values between 0.05 M and 0.3 M, solubility is no longer observed at low pH. Furthermore, as the concentration of NaCl increases, the pH at which the polymer phase separates decreases. Again, NaCl is acting to shield coulombic interactions (both attractive and repulsive) and to possibly enhance the hydrophobic effect. Recall that the homopolymer of **C(0:100)** has a CEC of 0.17 M NaCl; however, **C(25:75)** phase separates even in 0.3 M NaCl at pH 3.9. If the attractive coulombic interactions of **C(25:75)** were the *sole* cause of phase separation at low pH values, then one might expect the polymer solution to remain homogeneous at concentrations of NaCl above 0.017 M. Other factors, such as an increase in the hydrophobicity of the copolymer, are also operating, thus leading to phase separation. However, that attractive coulombic interactions are still influential in 0.3 M NaCl is supported by the observation that in 0.5 M NaCl, no phase separation is observed for **C(25:75)** over the entire pH range investigated. As the concentration of NaCl is increased to 0.5 M NaCl, the attractive coulombic interactions of the zwitterions are finally sufficiently disrupted and the enhanced hydration of the charged groups leads to complete solubility. There is also a polymer concentration dependency on the phase behavior of DABDAPS-25 (Table 5.2),

as different pH values are required for phase separation. This suggests that there may be specific interactions between DABDAPS-25 and sodium chloride.

**CsCl, NaBr, and NaSCN solutions**

Shown in Table 5.2 are the effects of selected electrolytes on the critical pH required for phase separation. The critical pH values reported for sodium chloride and cesium chloride are very similar. However, the cesium cation must be more influential than the sodium cation, as no phase separation is observed at low concentrations of added electrolyte. This behavior is not fully understood but may be due to preferential association with the anionic moieties of the polyzwitterion or water structuring. Greater effects on the critical pH value are observed for sodium bromide and sodium thiocyanate. This behavior is likely a result of two competing interactions. As noted for the CEC studies of **C(0:100)**, the larger more, polarizable anions require lower concentrations to solubilize the homopolymer. However, these counterions are also anticipated to bind more strongly with the quaternary ammonium group of **1** as it is converted from a zwitterionic moiety to a cationic moiety. In fact, Stejskal et al. have reported phase separation of polycations in the presence of KSCN.[13] The tighter counterion association leads to a decrease in hydration of these mer units resulting in enhanced hydrophobicity and, therefore, a decrease in the solubility of the polymer. For **C(25:75)**, the 'salting in' effect of the added electrolytes appears to be the more dominant factor imposing solubility. As the mol% of the carboxybetaine mer unit is increased, however, the enhanced counterion binding appears to lead to a decrease in solubility at low pH.

Table 5.3 indicates the phase behavior of **C(50:50)** as a function of pH in the presence of different electrolytes. In contrast to **C(25:75)**, no phase separation is observed in sodium chloride and cesium chloride solutions throughout the entire pH range. **C(75:25)** and **C(100:0)** were also soluble throughout the pH range in the presence of sodium chloride and cesium chloride. This behavior further supports the findings of Laughlin that the carboxybetaine mer unit is more hydrophilic or more strongly hydrated than the sulfobetaine mer unit.[12] Thus, for carboxybetaine mer units, attractive charge-charge and dipole-dipole interactions are overcome by the stronger interaction of the carboxylate group with water as compared to the sulfonate group. In the presence of larger anions, i.e. bromide and thiocyanate, phase separation is observed. As discussed above, specific counterion association of the small anion with the quaternary ammonium group of **1** as the pH is lowered would lead to a dehydration of the polymer chain and, as is observed, phase separation.

**Table 5.3. Phase Behavior of C(50:50) as a Function of pH[a]**

| Salt Concentration (M) | 0.02 g/dL | | | | 0.05 g/dL | | | |
|---|---|---|---|---|---|---|---|---|
| | NaCl | CsCl | NaBr | NaSCN | NaCl | CsCl | NaBr | NaSCN |
| 0.05 | - | - | - | $8.0^{ib}$ | - | - | - | $7.8^{ib}$ |
| 0.1 | - | - | $7.0^{ib}$ $4.0^{ia}$ | $7.7^{ib}$ | - | - | $6.4^{ib}$ | $5.7^{ib}$ |
| 0.3 | - | - | $3.0^{ib}$ | $3.8^{ib}$ | - | - | $2.9^{ib}$ | $3.4^{ib}$ |
| 0.5 | - | - | - | - | - | - | - | - |

[a] ib = insoluble below listed pH. ia = insoluble above listed pH. - = no phase separation observed between pH 1 and 13

The counterion association effects of the large anions at low pH is further evidenced by examining the phase behavior of all the copolymers in the presence of sodium thiocyanate (see Table 5.4). The competing effects of the enhanced solubility of the sulfobetaine mer units (recall that the CEC = 0.02 M NaSCN for **C(0:100)**) versus the reduced solubility of the carboxybetaine mer units in the cationic form are apparent. The higher the mol% of sulfobetaine mer units incorporated into the copolymer, the lower the concentration of sodium thiocyanate required to solubilize the copolymer. Furthermore, **C(100:0)**, the homopolymer of **1**, phase separates as the pH is lowered to ca. 4.4 regardless of the concentration of sodium thiocyanate.

**Table 5.4. Phase Behavior of C(X:Y) Copolymers in Varied Concentrations of NaSCN as a Function of pH[a]**

| Salt Concentration (M) | C(25:75) | C(50:50) | C(75:25) | C(100:0) |
|---|---|---|---|---|
| 0.05 | $7.0^{ib}$ | $7.8^{ib}$ | - | $4.3^{ib}$ |
| 0.1 | $4.0^{ib}$ | $5.7^{ib}$ | $7.3^{ib}$ | $4.4^{ib}$ |
| 0.3 | - | $3.4^{ib}$ | $7.4^{ib}$ | $4.4^{ib}$ |
| 0.5 | - | - | $4.7^{ib}$ | $4.4^{ib}$ |
| 0.8 | - | - | - | $4.4^{ib}$ |
| 3.0 | - | - | - | $4.4^{ib}$ |

[a] ib = insoluble below listed pH. - = no phase separation observed between pH 1 and 13

## CONCLUSION

The solubility behavior of the copolyzwitterion series was investigated as functions of copolymer composition, pH, and added electrolytes. **C(0:100)**, the homopolyzwitterion of the sulfobetaine monomer, was insoluble in deionized water and required the addition of a critical concentration of electrolyte for solubilization. Larger, more highly polarizable anions were more effective in solubilizing **C(0:100)** in accord with the Hoffmiester series for anions. **C(100:0)**, the homopolyzwitterion of the carboxybetaine monomer, is soluble in deionized water because of

the more hydrophilic nature of the carboxybetaine group. **C(25:75)** exhibited the most complex solubility behavior as a function of pH and added electrolytes. This behavior was interpreted as a competition of the attractive and repulsive coulombic interactions and hydrophobic effects caused by counterion association of small anions with the quaternary ammonium groups as pH was lowered. **C(50:50)**, **C(75:25)**, and **C(100:0)** remain soluble in the presence of chloride anions at all pH values investigated. In the presence of thiocyanate anions, however, these polymers phase separate at a critical pH and electrolyte concentration. **C(100:0)** precipitated at a pH ca. 4.4 regardless of the concentration of NaSCN. This behavior has been attributed to tighter counterion binding of the thiocyanate anions along the polycation chain resulting in dehydration and ultimately phase separation.

## REFERENCES


1. McCormick, C. L.; Johnson, C. B. *Macromolecules*, **21**, 687 (1988).

2. McCormick, C. L.; Johnson, C. B. *Macromolecules*, **21**, 694 (1988).

3. McCormick, C. L.; Salazar, L. C. *Polymer*, **33**, 4384 (1992).

4. McCormick, C. L.; Salazar, L. C. *Polymer,* **33**, 4617 (1992).

5. McCormick, C. L.; Salazar, L. C. *Macromolecules*, **25**, 1896 (1992).

6. McCormick, C. L.; Salazar, L. C. *J. Appl. Poly. Sci.*, **48**, 1115 (1993).

7. Salamone, J. C.; Volksen, W.; Israel, S. C.; Olson, A. P.; Raia, D. C.; *Polymer*, **18**, 1058 (1977).

8. Monroy Soto, V. M.; Galin, J. C. *Polymer*, **25**, 121 (1984).

9. Monroy Soto, V. M.; Galin, J. C. *Polymer*, **25**, 254 (1984).

10. Higgs, P. G. and Joanny, J. F., *J. Chem. Phys.*, **94**, 1543 (1991).

11. Schulz, D. N.; Peiffer, P. K.; Agarwal, J.; Larabee, J.; Kaladas, J. J.; Soni, L.; Handwerker, B.; Garner, R. T. *Polymer*, **27**, 1734 (1986).

12. Salamone, J. C.; Quach, L.; Watterson, A. C.; Krauser, S.; and Mahmud M. U. *J. Macromol. Sci., Part A*, *22*, 653 (1985).

13. Corpart, J.; Candau, F. *Macromolecules* , **26**, 1333 (1993).

14. Skouri, M.; Munch, J. P.; Candau, S. J.; Neyret, S.; Candau, F. *Macromolecules* , **27**, 69 (1994).

15. Peiffer, D. G.; Lundberg, R. D. *Polymer*, **26,** 1058 (1985).

16. Liaw, D. J.; Lee, W. F. ; Whung, Y. C.; Lin, M. C. *J. Appl. Polym. Sci.*, **37**, 999 (1987).

17. Salamone, J. C.; Volksen, W.; Israel, S. C.; Olson, A. P. *Polymer*, **19**, 1157 (1978).

18. Schulz, D. N.; Kitano, K.; Dannik, J. A.; Kaladas, J. J. *Polym. Mater. Sci. Eng.*, **147**, 149 (1987).

19. Ladenheim, H.; Morawetz, H. *J. Polym. Sci.,* **26***(113)*, 251 (1957).

20. Topichiev, D. A.; Mkrtchyan, R. A.; Simonyan, R. A.; Kabanov, V. A. *Polym. Sci., U.S.S.R. (Eng. Transl.)*, **A19**, 580 (1977).

21. Wielma, T., *PhD Dissertation*, University of Groningen, 1989.

22. Laughlin, R.G. *U.S. Patent 4,287,174*, **1981**.

23. Chevalier, Y.; Storet, Y.; Pourchet, S.; LePerchec, P. *Langmuir,* **7**, 848 (1991).

24. Weers, J. G.; Rathman, J. F.; Axe, F. U.; Crichlow, C. A.; Foland, L.D.; Scheuing, D. R.; Wiersema, R.J.; Zielske, A. G. *Langmuir,* **7**, 854 (1997).

25. McCormick, C.L.;Salazar, L.C *J. Polym. Sci., Part A*, **31**, 1099 (1993).

26. McCormick, C.L.;Blackmon, K.P. *Polymer,* **27**, 1971 (1986).

27. Fineman, M.; Ross, S. *J. Polym. Sci.*, **5**, 259 (1950).

28. Kelen, T.; Tudos, F. *J. Macromol. Sci., Chem.,* **A9**, 1 (1975).

29. Tidwell, P. W.; Mortimer, G. A. *J.Polym. Sci.:Part A*, **3**, 369 (1965).

30. Igarashi, S. *J. Polym. Sci., Polym. Lett. Ed.*, **1**, 359 (1963).

31. Salamone, J. C.; Ahmed, I.; Rodriguez, E. L.; Quach, L.; Watterson, A. C. *J. Macromol. Sci. Chem., Part A*, **25**, 811 (1988).

32. Laughlin, R.G. In *Advances in Liqid Crystals*; Brown G.H.,Ed.; Academic Press: New York, **1978**; *Vol. 3*, p41 and p99.

33. Collins, K.D.; Washabaugh, M. W. *Quat. Rev. of Biophys.*, **18(4)**, 323 (1985).

34. Molyneux, P. Water-Soluble Synthetic Polymers: Properties and Behavior, Vol. II; CRC Press: Boca Raton, FL., 1984.

35. Yasuzawa, M., Nakaya, T., and Imoto, M., *J. Macromol. Sci. Chem. Part A*, **23(8)**, 963 (1986).

36. Pujol-Fortin, M. L. and Galin, J. C., *Polymer,* **35**, 1462 (1994).

37. Ladenheim, H. and Morawetz, *J. Polym. Sci.*, **26**, 251 (1957).

38. Rosenheck, K. and Katchalsky, A, *J. Polym. Sci.*, **32**, 511 (1958).

39. Topchiev, D. A., Mkrtchyan, L. A., Simonyan, R. A., Lachinov, M. B., and Kabanov, R. A., *Polym. Sci. U.S.S.R. (Eng. Transl.)* **A19**,580 (1977).

40. (a)Wielema, T. A. and Engberts, J. B. F. N., *Eur. Polymer J.,* 1**988**, *24*, 647. (b) Wielma, T.A. PhD Dissertation, University of Groningen, 1989.

41. Hsu, Y. G., Hsu, M. J., Chen, K. M., *Makromol. Chem.*, **192**, 999 (1991).

42. (a) Kathmann, E. E. and McCormick, C. L., *Polym. Prepr. Am. Chem. Soc. Div. Polym. Chem.* **35(2)**, 641 (1994). (b) Kathmann, E. E., White, L. A., McCormick, C. L., *Polymer,* **38(4)**, 879-886 (1997).

43. McCormick, C.L.;Salazar *J. Polym. Sci., Part A*, **31**, 1099 (1993).

44. McCormick, C.L.;Blackmon, K.P. *Polymer,* **27**, 1971 (1986).

45. Collins, K.D.; Washabaugh, M. W. *Quat. Rev. of Biophys.*, **18(4)**, 323 (1985).

46. Laughlin, R.G. In *Advances in Liqid Crystals*; Brown G.H.,Ed.; Academic Press: New York, 1979, Vol 3, p.41 and 99

49. McCormick, C. L.; Elliott, D. L. *Macromolecules,* **19**, 687 (1986).

50. McCormick, C. L.; Newman, J. K. *Macromolecules,* **27**, 5114 (1994).

49. Stejskal, J.; Benes, M. I.; Kratochvil, P. *J. Polym. Sci., Polym. Phys. Ed.*, **12**, 1941 (1974).

# CHAPTER 6. CAPILLARY RHEOMETER DESIGN AND OPERATION

## INTRODUCTION

Current research in our laboratories is focused on the use of polymer additives for fluid mobility control in flow through porous media. The flow field in porous media contains frequent accelerations and decelerations as the fluid passes through channels of varying size. The changing fluid velocity results in extensional and compressional strains on the fluid. Since polymer coils in solution exhibit significant resistance to extension and compression, polymer solutions show a decrease in mobility through porous media as compared to pure solvent.

Past observations [1,2] indicate that a polymer coil's hydrodynamic volume in solution is strongly related to its effectiveness for mobility control. Polymer hydrodynamic volume is proportional to the product of intrinsic viscosity and molecular weight. Intrinsic viscosity increases with increased solvent-polymer thermodynamic interactions. Thus, a good candidate for mobility control in flow through porous media is a polymer that is highly solvated by the solvent at the applied conditions.

In the application of enhanced oil recovery (EOR), the polymer solution temperature is elevated as it flows into the oil reservoir. Ideally, a polymer used in EOR should become more solvated with increases in temperature. The degree of solvation in any environment is proportional to the intrinsic viscosity of the polymer in that environment. Therefore, it is extremely important to be able to measure the intrinsic viscosity over a range of conditions. Thus, efforts have been directed at experimentally measuring the intrinsic viscosities of polymer solutions over a range of temperatures and solvent compositions typically found during polymer flooding of oil reservoirs.

### Difficulties with high temperature solution viscosity measurement

Several problems arise when measuring intrinsic viscosities of high molecular weight polymer solutions at elevated temperatures. The small shear rates and low concentrations necessary for accurate intrinsic viscosity determination result in very small shear stress forces that must be measured. In the past, a Contraves LS-30 low shear rheometer has been used to determine intrinsic viscosities at room temperature. Although the instrument can heat the fluid being measured, the elevated temperatures cause solvent evaporation from the polymer solutions. Because the Contraves uses a small sample volume (less than 5 mL), loss of a small amount of solvent can cause noticeable concentration changes leading to large error in intrinsic determination. In addition, the solvent vapors are funneled up into the optical sensor/electronics carriage located above the sample causing noise and possible damage to the very sensitive instrument. For these reasons the Contraves LS-30 is not suitable for determining high temperature intrinsics.

Another problem exists with making high temperature fluid property measurements. Aqueous solutions that are prepared at room temperature and then heated will de-gas because air becomes less soluble at elevated fluid temperatures. This causes air bubbles to form in the solutions as fluid temperature is elevated, adversely affecting experimental measurements. To prevent this problem, the solutions must be de-gassed prior to analysis by heating with agitation to or beyond the experimental temperature.

Finally, the problem of finding an apparatus sensitive enough to detect the small forces generated

during dilute polymer solution intrinsic viscosity determination at low shear rates is compounded at high temperatures. As the temperature is increased, the viscosity of the solvent, water, decreases drastically. For example, the viscosity of a very dilute solution is effectively halved when the solution is heated from 20°C to 55°C, thus reducing the shear stress forces generated by a factor of two. No commercially available instrument is capable of making the low force measurements; therefore, a new steady shear rheometer has been designed and constructed in our laboratory for this purpose.

## CAPILLARY RHEOMETER DESIGN AND CONSTRUCTION

Laminar flow through a small tube or capillary is governed by the Hagen-Poiseullie relationship.

$$Q = \frac{\pi D^4 \Delta P}{128 L \eta_{app}} \qquad \text{Hagen-Poiseullie Equation}$$

If a fluid is forced through a capillary of known length L and diameter D at a known flow rate, Q, then the apparent viscosity of the fluid, $\eta_{app}$, can be calculated if the fluid pressure drop across the capillary, $\Delta P$, can be measured. The shear rate, $\dot{\gamma}$ , for capillary flow can also be calculated knowing capillary geometry and the fluid flow rate ( $\dot{\gamma} = 32 Q / \pi D^3$ ). Since a capillary tube can be considered as a long cylindrical dye, the Hagen-Poiseullie Equation equation can be rearranged in the form of the die equation ($Q = k \Delta P / \eta_{app}$) where k is the cylindrical die constant and is a function only of the geometry ($k = \pi D^4 / 128 L$).

The rationale for designing the new capillary rheometer was to establish a steady, controlled fluid flow at low shear rates, less than 10 $sec^{-1}$, through a small diameter tube and to accurately measure the resulting pressure drop across the tube. The long tube was to be coiled and submersed in a controlled temperature bath providing a means for high temperature fluid viscosity measurements. The design requirements are not easily satisfied. The fluid flow-rate must be small enough and/or the tube diameter large enough to meet the low shear rate requirement. Also the tube must be long enough to give a pressure drop sufficient for detection. Finally, both the tube diameter and length must be small enough to render a reasonable fluid sample volume for convenient experimentation.

The ISCO model 500D syringe pump, already used for extensional viscosity measurements in the SER, was chosen to produce the required steady fluid flow rate through the tube. The pump can maintain steady and pulseless flow in the range of 200 mL/min to 0.001 mL/min with 0.5% accuracy.

Initially, an Entran model EPE-V21-2P pressure transducer with a range of 2 psi was used to measure the fluid pressure drop across the tube. The pressure sensing diaphragm in this device was a monolithic silicon chip which was sensitive to direct contact with water. Since the transducer is placed in direct contact with a dilute aqueous solution during operation, problems with drift in the output voltage signal were observed. This problem was corrected by replacing the transducer with an Entran model EPX-V01-10P transducer having a range of 10 psi. The new device has a 304 stainless steel diaphragm which is not water sensitive.

The dimensions of the capillary tube were designed to make the best use of the syringe pump and pressure transducer. The material chosen for tube construction was nickel due to its high resistence to corrosion, especially by salt solutions. The specifications of the capillary tube are given in Table 6 .1 below. For this capillary, a volumetric flow-rate of 0.037 mL/min is required to achieve the same low shear rate present in the Contraves rheometer, 6 $sec^{-1}$. Using the Hagen-Poiseullie equation, water at 20°C would produce a pressure drop across the tube of 0.5 psi under these flow conditions, well within the range of the selected pressure transducer.

**Table 6.1.** Specifications of capillary tubing used in rheometer.

| Supplier | Material | I.D. | O.D. | Length | Internal Volume |
|---|---|---|---|---|---|
| Valco Instruments part no. TNI 140 | nickel | 0.040 in | 1/16 in | 530 ft | 131 mL |

The capillary rheometer plumbing system consists of zero dead-volume stainless steel valves and stainless steel tubing (see Figure 6.1). The syringe pump fluid output is routed through a two-way valve allowing flow to be switched between the screen extensional rheometer and the capillary rheometer. The capillary flow line then contains a tee where the pressure transducer is installed. A two-way valve is used to isolate the transducer before fluid is put under any high pressures that would damage the transducer. Chapter 7 discusses the dynamic calibrating procedure used to convert transducer voltages to fluid pressures.

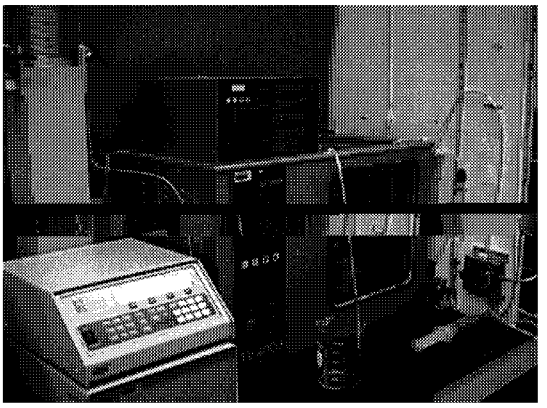

**Figure 6.1**. Capillary rheometer

Downstream of the tee, the flow line goes through a four-way valve which provides a means for cleaning the capillary. In one valve position, the capillary is inline with the pump, while in the other position, it is connected to a high pressure cylinder. This cylinder can be filled with water, acetone, or any other solvent and subsequently pressurized with nitrogen. The cleaning solvent can thus be forced through the capillary followed by clean dry nitrogen. In this manner, the capillary can be cleaned at high pressure, requiring less time for the solvent to flow through its extensive length. The capillary tube itself is a 10 inch diameter coil that is submerged in a Tamson model TV 4000 water bath as shown in Figure 6.2. The downstream end of the tube is open to the atmosphere so that one pressure transducer at the tube fluid inlet is sufficient for obtaining the pressure drop across the capillary.

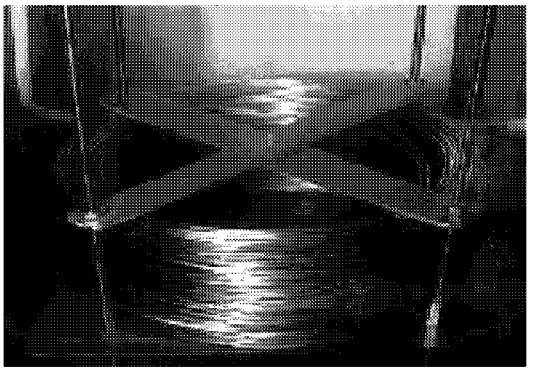

**Figure 6.2**. Coiled nickel tubing in bath.

## CAPILLARY RHEOMETER OPERATION

Operation of the capillary rheometer consists of a few simple steps. The water bath is set to the desired temperature. The syringe pump is loaded with approximately 250mL of the de-gassed fluid sample. Fluid de-gassing is discussed in Chapter 7. With the pressure transducer off-line, the fluid is pumped into the capillary at a flow-rate sufficiently low to ensure laminar fluid flow conditions (about 30 mL/min). Once the 131mL capillary volume has been filled with fluid, additional fluid is pumped through the tube to ensure that the fluid previously in the tube has been flushed out and only new sample fluid is present (about 200mL total). Flow from the pump is then stopped, and the transducer voltage is adjusted to zero. Thereafter the flow rate is adjusted to that needed to achieve the target shear-rate. Once the system has equilibrated (about 2 minutes) the pressure transducer is switched online and the output voltage is collected in real-time by National Instruments LabView data acquisition software, the same software that is used to collect data for the screen extensional rheometer. After sufficient pressure versus flow-rate data has been collected, the pressure transducer is switched offline and the remaining sample is removed from the pump, making the pump ready for the next fluid. After all fluid samples have been run, the pump cylinder is flushed with several volumes of pure water and thereafter with nitrogen gas, thus cleaning and drying the capillary.

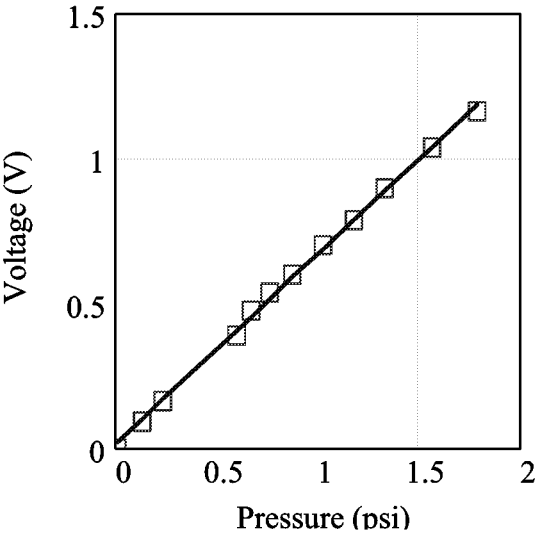


**Figure 6.3.** Voltage output vs. pressure for the Entran transducer with fit line.

### Data Interpretation

By measuring the transducer voltages for pure solvent and for a series of polymer solutions flowing through the capillary rheometer, Huggins and Kraemer plots can be generated to determine intrinsic viscosity. Solution pressure drops are calculated from transducer voltages and a calibration curve (see Figure 6.3). Also, pressure drop vs. flow rate measurements have been made at four temperatures with water, for which the fluid viscosity is known. The die constant, k, has been determined according to the die equation ( $k = \eta_{app} Q / \Delta P$ ) for each of these temperatures and is shown in Table 6.2 along with the theoretical k calculated from die geometry. Using this constant, the apparent viscosity of a fluid can be determined directly from the flow-rate and pressure drop ($\eta_{app} = k \Delta P / Q$).

**Table 6.2.** Instrument constant ($cm^3 \times 10^{10}$).

| k from theory | k at 1°C | k at 20°C | k at 60°C | k at 80°C |
|---|---|---|---|---|
| 1.62 | 1.58 | 1.62 | 1.52 | 1.66 |

**Initial Capillary Rheometer Experimentation**

Several experiments were performed with deionized water at different temperatures in order to determine the response characteristics, sensitivity, and consistency of the instrument. The capillary was loaded with water and then flow was stopped. The pressure transducer was then adjusted to read zero voltage at zero flow-rate. A series of step changes in the flow-rate were then performed, and the instrument's pressure response was measured in real-time by the transducer via LabView software. When a fluid flow-rate step change is input, the pressure output is a first order exponential response as in Figure 6.4. The output data was curve-fitted accordingly to reveal the characteristic response time. A short response time is desirable since each data point in an actual experiment should be taken after flow equilibrium has been established. If the instrument responds too slowly, the time of experimentation could be unreasonably long. The curve fit also yields the final value that the voltage should reach after infinite time. The final signal values were used to calculate the noise to signal ratio of the instrument at several temperatures and shear rates. Although the noise (standard deviation of voltage values) to signal (mean of voltage values) ratio varied slightly from one experiment to another, it was generally less than 1%.

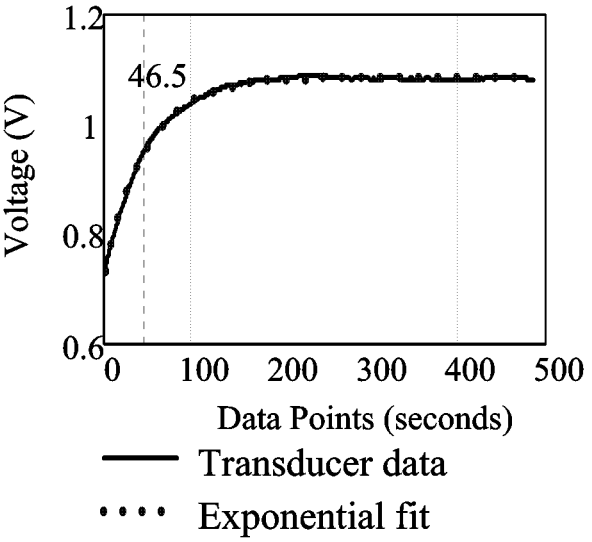


**Figure 6.4.** Typical rheometer response to an input step change in flow-rate. The characteristic time is 46.5 seconds.

One factor found to affect the characteristic response time of the capillary rheometer was the presence of air bubbles in the fluid. This suspicion was confirmed by deliberately introducing small amounts of air into the fluid within the capillary and analyzing its effect. The instrument response time increased greatly (~ 10 fold) when air bubbles were present. Therefore, care must be taken to ensure that no air is introduced into the fluid during operation. De-gassing the fluids before experimentation is essential to reducing signal noise and minimize the time of experimentation.

An experiment was performed to justify one aspect of the operating procedure. After data for a fluid sample has been collected and the remaining fluid ejected from the syringe pump, the capillary is still full of this sample. Since the fluid experiences laminar flow during sample loading, it was assumed that there is nearly plug-like displacement of an old fluid sample when a new sample is forced through the capillary tube. If this assumption is true, then the capillary does not need to be emptied and extensively cleaned between solutions, and the time of experimentation can be reduced. To test this idea, the capillary was filled with pure water. The pump was then loaded with water containing red food coloring. The "red water" was pushed through the capillary displacing the pure water as it proceeded. If back-mixing occurred, the water exiting the tube would turn pink before the 131 mL tube volume had been pumped through. The fluid began to turn pink after 128 mL and was completely red by 134 mL. This indicated that there was a 6 mL window of mixed fluids. In actual experimentation 60 to70 mL of extra fluid are pumped through the tube. This should be more

than enough fluid to eject any mixed sample within the tube and thus ensure that only the new fluid sample is present within the capillary tube.

In initial tests, the capillary rheometer has been used to measure the intrinsic viscosity of a poly(ethylene oxide) solution. Poly(ethylene oxide) (Polyox® WSR-301 4.1 million mol. wt.) solution viscosities were determined using the capillary rheometer at 22 °C and at a shear rate of 6 $s^{-1}$ and compared with solution viscosity data obtained from the Contraves LS-30. The results of these measurements are shown in Figure 6.5.

The resulting intrinsic viscosity from the capillary rheometer agrees closely with the value obtained from the Contraves (see Table 6.3). The fact that the solution intrinsic viscosity is slightly higher for the capillary rheometer may be explained by the small fluid temperature difference when operating the two instruments. These results suggest that the capillary rheometer may indeed be a viable means for determining intrinsic viscosities of high molecular weight polymers in aqueous solutions.

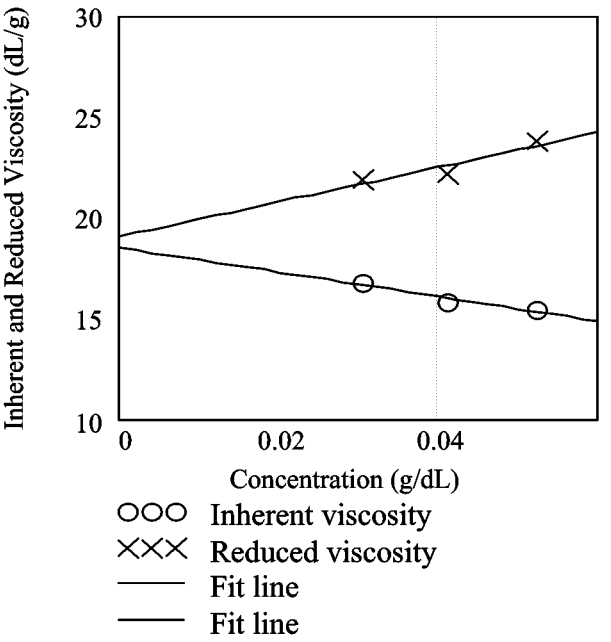


**Figure 6.5.** Huggins and Kraemer plots for 4.1 million mol. wt. PEO in DI water at 22 °C.

**Table 6.3.** Intrinsic viscosity data comparison for 4.1 million mol. wt. poly(ethylene oxide).

| Property | Units | Value |
|---|---|---|
| Intercept $_{reduced}$ | dL/g | 19.1 |
| Correlation coefficient | | 0.933 |
| Intercept $_{inherent}$ | dL/g | 18.5 |
| Correlation coefficient | | 0.954 |
| $[\eta]_{average}$ at 22 °C | dL/g | 18.8 |
| $[\eta]_{Contraves}$ at 25 °C | dL/g | 18.6 |

## CONCLUSIONS

The intrinsic viscosity of a high molecular weight polymer aqueous solution is difficult to measure due to the low concentrations and low shear rates required to perform the experimentation. This difficulty is compounded at high temperatures by concentration changes due to solvent evaporation and by decreased solvent viscosity. Intrinsic viscosity, however, is a very important parameter in polymer solution rheology and must be measured at conditions experienced during

enhanced oil recovery, such as elevated temperatures.

A new capillary type, low shear rheometer has been designed and constructed in our laboratory for the purpose of determining polymer solution intrinsic viscosity at elevated temperatures. The instrument is capable of detecting the small forces produced when low viscosity fluid are subjected to low shear rates. The entire capillary can be submerged in a heated bath, and, since it is a closed system, there is no solvent loss during experimentation. Instrument performance and sensitivity have been evaluated over a range of temperatures with promising results. The rheometer has also been used to determine the intrinsic viscosity of a poly(ethylene oxide) solution and is in good agreement with the value obtained using a Contraves LS-30 cup and bob type rheometer.

New macromolecules are being developed in our laboratories for possible use in polymer flooding of oil reservoirs. The capillary rheometer will be used to determine the intrinsic viscosities of these polymers in aqueous solution at various temperatures and solvent compositions, i.e. presence of electrolytes. After the intrinsic viscosity of a polymer in a particular solution environment is evaluated in the laboratory, its performance in oil reservoir flooding can be more accurately estimated.

## REFERENCES


1. McCormick, C. L. and R. D. Hester, *Responsive Copolymers for Enhanced Petroleum Recovery, Annual Report,* June 2000 (DOE/BC/15111-1).

2. McCormick, C. L. and R. D. Hester, *Responsive Copolymers for Enhanced Petroleum Recovery, Annual Report,* February 2001 (DOE/BC/15111-2).

# CHAPTER 7. SOLUTION VISCOSITIES AT ELEVATED TEMPERATURES

## INTRODUCTION

As previously discussed in Chapter 6, a low-shear capillary viscometer has been designed and implemented for the determination of intrinsic viscosities of high molecular weight polymers in aqueous solution over a range of temperature. A reliable method for solution preparation and a method for the acquisition and analysis of capillary flow data were perfected so that accurate intrinsic viscosity information can be obtain. This work is discussed below.

## POLYMER SOLUTION PREPARATION

The first step in determining dilute polymer solution properties is to prepare a concentrated stock solution. To prevent biological growth in the solutions and increase the shelf life, all solvents are treated with 100 ppm sodium azide. Whether obtained commercially or synthesized in our laboratory, the polymer samples for rheological characterization are received in solid form. The water soluble polymers are highly hygroscopic, capable of absorbing significant amounts of water from the surrounding air. Absorbed water poses a potential problem in solution preparation because the solid polymer mass can be comprised of as much as 10 to 30 wt. % water.

### Concentrated Solutions

An accurate calculation of solution concentration requires an accurate measurement of the mass of *dry* polymer dissolved in the solvent. In the past, a polymer sample was dried overnight under vacuum at a temperature low enough to avoid degradation (about 40°C). The *dry* polymer was then sealed and quickly transferred to a balance for weighing. The balance, accurate to 0.0001 gram, was loaded with trays of NaOH pellets to absorb any ambient moisture in the weigh chamber. Finally, the polymer sample was weighed and added to a known mass of appropriate solvent, yielding a concentrated stock solution.

An alternate method of obtaining the weight of dry polymer has been employed more recently. A deliberate amount of the *wet* polymer sample (solid polymer that has reached an equilibrium moisture content) is weighed to 0.0001 grams and added to a known mass of solvent (pre-filtered to remove dust). Meanwhile, a second small portion of the same solid polymer sample is weighed into a tarred vial with a cap. The vial is then loosely covered and dried under vacuum overnight as before. Once the oven has cooled under vacuum, the vial is immediately capped and re-weighed. The weights before and after drying (less the weight of the vial and cap) are used to find the moisture content of the original sample. The weight of polymer in the stock solution is adjusted for the percent moisture to obtain the weight of dry polymer for the purpose of calculating solution polymer concentration.

### Solution Dilution

Intrinsic viscosity determination requires a series of dilute solutions over some range of polymer concentrations. After a stock solution has been prepared and its concentration is accurately known, it is a trivial task to further dilute the solution to any desired lower concentration. A far more

uncertain experimental step concerns determining which polymer concentrations to prepare to find the intrinsic viscosity. In order to avoid chain entanglements and yield a reliable extrapolation to zero concentration, all dilute polymer solutions should be below the critical overlap concentration, $c_{star}$. The parameter $c_{star}$ can be approximated as the condition where $c\,\eta_{intr} = 1$. Solutions for characterization in the screen extensional rheometer (SER) are considered dilute when the concentration is $c_{star}/10$; that is $c\,\eta_{intr} = 0.1$ where c is concentration in g/dL, and $\eta_{intr}$ is intrinsic viscosity in dL/g. However, the polymer intrinsic viscosity must be known before a solution that meets this criteria can be prepared. Therefore, a reasonable initial estimate of intrinsic viscosity is necessary to ensure that dilute solution concentrations prepared are in the appropriate range when making the solution viscosity measurements needed to calculate the intrinsic viscosity.

When a polymer of unknown intrinsic viscosity is received for rheological characterization, a concentrated stock solution is prepared as described above and several dilutions are made over a wide range of concentrations. These are analyzed in the capillary viscometer to develop a preliminary estimate of the intrinsic viscosity at some chosen solvent conditions. Inevitably, some of the solutions will be too concentrated (above $c_{star}$) and some too dilute (indistinguishable from pure solvent), but the experiment will enable the selection of the range of concentrations to prepare for future measurements. Once $c_{star}$ has been estimated, several (usually 5) dilute solutions are made from a stock concentrated solution. The apparent viscosities of the dilute solutions as well as the pure solvent are measured with the capillary viscometer as described below. The intrinsic viscosity is then calculated for the polymer solvent system using the solution viscosities determined in the capillary rheometer. Finally, a solution for use in the SER is prepared such that the polymer concentration is equal to $c_{star}/10 = 0.1 / \eta_{intr}$.

**Final Solution Preparation**

Once the proper dilutions have been made for a particular polymer solvent system, the dilute solutions are agitated on an orbital shaker until polymer dissolution is complete and the solution reaches a state of homogeneity. The solution rheological property studies are performed at different temperatures. As reported in Chapter 6, experiments at elevated temperatures require that the solutions first be de-gassed. De-gassing of a solution is done just prior to the particular high temperature experiment. The solution-containing vessel (usually an Erlenmeyer flask) is immersed in a heated water bath and agitated by a magnetic stir bar. In this way, the solution is heated a few degrees beyond the temperature of the planned experiment. Gasses that were dissolved in the fluid are liberated as their solubility is decreased. Agitation assists the gasses to bubble out and escape through a vent in the stoppered vessel. At this point, the dilute polymer solution is ready to be examined in the capillary viscometer or screen extensional rheometer.

## SOLUTION VISCOSITY DATA ACQUISITION

The capillary viscometer and basic procedures used to make the measurements necessary for intrinsic viscosity determinations was described in Chapter 6 . The steps involved in loading and unloading a polymer solution have not been altered. The method of acquiring the raw data and processing the raw data into fluid shear viscosities and intrinsic viscosities is discussed below.

### Operational Procedures

The first step in intrinsic viscosity determination is to measure the apparent viscosity of the pure solvent. The pressure drop required to load the capillary with fluid in a timely manner (several hundred psi) is high enough to damage the diaphragm of the low pressure transducer; therefore, the transducer is switched offline via a two-way valve during loading. Solvent is pumped into the capillary and then flow is halted. When the syringe pump is stopped, the pressure in the capillary tube decreases exponentially. After a few seconds, the pressure becomes low enough that the low pressure transducer can safely be switched online, and data acquisition is initiated. The system is allowed to come to equilibrium, at which time the pressure in the capillary and, consequently, the transducer output signal becomes constant. The signal conditioner is then "zeroed" or adjusted so that the output signal is zero volts at zero flow rate. The pump is set for the desired volumetric flow rate and solvent flow is started. The pressure in the capillary tube exponentially approaches a steady state value as indicated by the transducer voltage signal. Once the system approaches equilibrium (voltage becomes constant), a step change in flow rate is made via the pump controller. The system then approaches a new equilibrium pressure. In this way, voltage versus flow rate data is obtained for as many shear rates as desired. Upon completion of this process, flow is stopped and the raw data file is saved for later analysis.

The voltage versus flow rate data for the solvent is used to calculate a pressure transducer calibration function as described below. The solvent calibration allows determination of the apparent viscosities of a series of dilute polymer solutions. Each solution is loaded into the capillary and the data acquisition steps described above are repeated with the exception of zeroing the signal. The transducer has already been zeroed and calibrated so it is not necessary to re-zero for the remainder of the experiment. Data is collected for each solution under the same set of shear rates so that an extrapolation to zero shear rate can be preformed later.

## CAPILLARY VISCOMETER DATA ANALYSIS

### Raw Data

Raw data from the capillary viscometer is provided as an array of transduced voltage values. The voltage values or signals are acquired each second after a steady fluid volumetric flow rate through the capillary is initiated at time $t_{start}$. The first voltage value in the data array is the voltage at the time steady fluid flow was started or changed. Thereafter, signals are recorded each second for about five minutes or until a steady state condition has been approached.

### Signal Equilibrium

A plot of the voltage signal versus time always shows that the voltage signal increases with time after flow was initiated but eventually reaches a steady state value. This final steady state signal is the voltage value that can be associated with the fluid apparent viscosity at the given flow rate conditions. The exponential function given below as Equation (1) can be fitted to the voltage versus time data to find the final steady state voltage signal, $V_{final}$.

$$V = \frac{(V_{start} - V_{final})}{\exp\left[\frac{(t - t_{start})}{\lambda}\right]} + V_{final} \qquad (1)$$

In Equation (1), V is the voltage at time t, $t_{start}$ is the time fluid flow through the capillary was started, $\lambda$ is proportional to an instrument response time, and $V_{start}$ is the voltage when the time is $t_{start}$.

A nonlinear fitting routine, such as the Newton-Raphson-Marquart steepest decent method[1], can be used to determine parameters $\lambda$, $V_{start}$, and $V_{final}$ from a regression of the voltage verses time data set to the exponential function. A typical plot of the raw data and the exponential function fit curve is shown in Figure 7.1. Values for $t_{start}$, $V_{start}$, and $V_{final}$ are also shown. Note that the exponential function fits the experimental data very well. The correlation coefficient between the experimental voltages and the corresponding fit function voltage values (usually more than 300 data pairs) is almost always greater than 0.999. The fit line is so close to the data points that the data points are almost not visible in the plot.

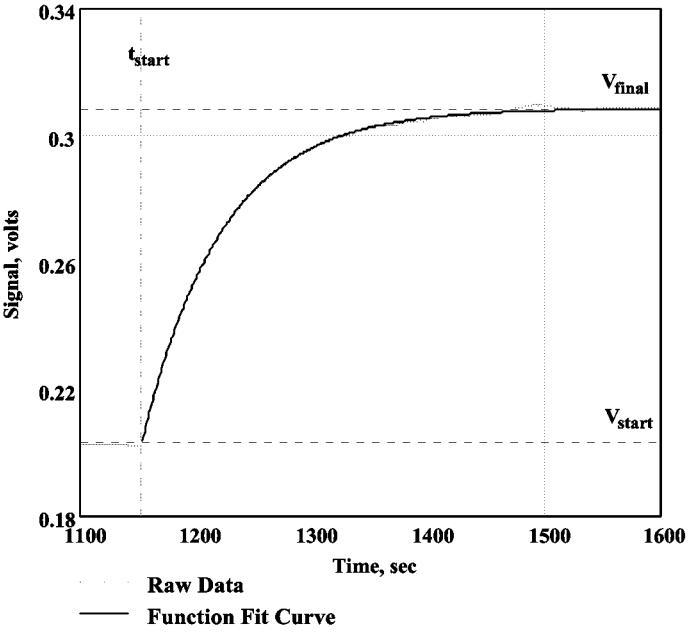


**Figure 7.1.** Typical Raw Data Plot and Fit Function Curve

**Transducer Calibration**

Before a set of polymer solution viscosities are measured by the capillary viscometer, the transducer used to measure the pressure drop across the capillary must be calibrated. This calibration is accomplished by flowing a Newtonian solvent having a known viscosity, $\mu_o$, (usually water or brine) through the capillary at various volumetric flow rates, Q. The final steady state voltage signals, $V_{final}$, at each flow rate are recorded. Because fluid flow within the capillary is laminar and the solvent viscosity is therefore unaffected by the fluid shear rate within the capillary, the Hagen-Poiseuille Equation[2], shown below, can be used to calculate the pressure drop across the capillary, $\Delta P$, at each flow rate.

$$\Delta P = \frac{8 L Q \mu_o}{\pi R^4} \qquad (2)$$

In Equation (2), R and L are the capillary inside radius and length, respectively. A plot of the fluid pressure drops versus corresponding steady state transducer voltages produces a calibration plot as shown in Figure 2. The data on the calibration plot can be fit to a straight line function. The intercept, A, and slope, B, of the line defines the transducer's dynamic calibration function, Equation (3). This equation relates a fluid pressure drop to a voltage signal.

$$\Delta P = A + B\,(V_{final}) \qquad (3)$$

Note that although the voltage signal was zeroed at zero flow rate, the intercept value, A, is not necessarily zero.

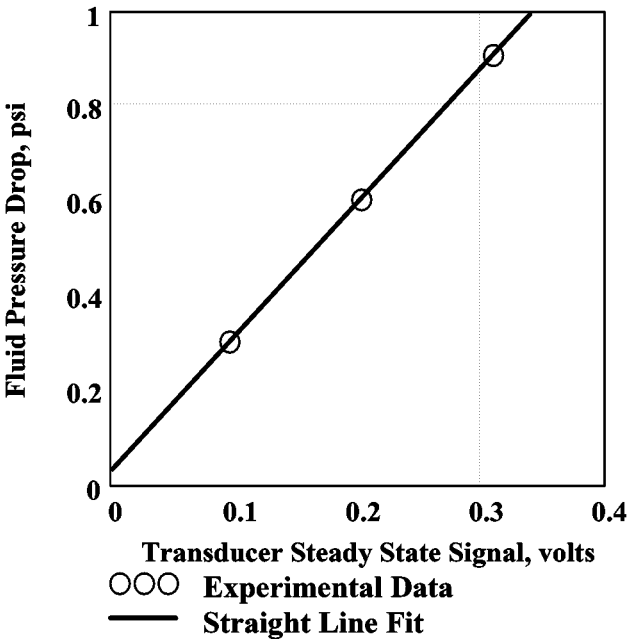


**Figure 7.2.** Typical Transducer Calibration Plot

Equation (3) can be used to determine the pressure drop for a polymer solution from the steady state transducer voltage signal. As shown by Equation (4), having the calibration function enables the use of a rearranged Hagen-Poiseuille Equation to calculate the solution apparent viscosity, $\eta$, at the given fluid flow conditions when the final steady state transducer voltage, $V_{final}$, is known.

$$\eta = \frac{\pi R^4 (\Delta P)}{8 L Q} = \frac{\pi R^4 (A + B V_{final})}{8 L Q} \qquad (4)$$

Using the above technique, the apparent solution viscosity, $\eta$, can be determined for each shear rate at which capillary flow data was collected. In general, a dilute polymer solution's apparent viscosity will decrease as the fluid flow rate increases and the first Newtonian shear viscosity or "zero" shear viscosity must be determined. This dependence of a solution's apparent viscosity on the flow rate is considered below.

**Solution "Zero" Shear Viscosities**

Because dilute polymer solutions are usually non-Newtonian and their apparent viscosities decrease with increasing shear rate, an extrapolation of solution apparent viscosities to a "zero" shear rate limit must done to find the solution's "zero" shear viscosity, $\eta_o$. As shown by Equation (5), the fluid shear rate at the wall, $\dot{\gamma}$ , in laminar flow through a capillary is directly proportional to the flow rate, Q.

$$\dot{\gamma} = \frac{4Q}{\pi R^3} \qquad (5)$$

For dilute polymer solutions the apparent shear viscosity is expected to decrease with increasing shear rates as described by the Bueche rheological function[3], Equation (6). A dilute polymer solution is a solution in which the flow behavior of individual polymer macromolecules in the solution is not affected by any surrounding polymer macromolecules.

$$\frac{\eta - \mu_o}{\eta_o - \mu_0} = 1 - \sqrt{\phi\ \dot{\gamma}} \qquad (6)$$

In Equation (6) $\phi$ is a time that characterizes the motion of a polymer coil in a solution. $\phi$ is expected to increase as the polymer coil size increases. The coil size increases as the polymer molecular weight increases, as the polymer is more solvated by the solvent and as the flexibility of the macromolecule decreases. The Bueche Equation can be rearranged into a linear relationship as shown by Equation (7).

$$\eta = \eta_o - (\eta_o - \mu_o)\sqrt{\dot{\gamma}}\ \sqrt{\phi} \quad (7)$$

Therefore a linear fit of the solution apparent shear viscosities verses the square root of corresponding shear rates should give an intercept, a, that is equal to the solution's "zero" shear rate viscosity, $\eta_o$, and a slope b that is equal to $(\eta_o - \mu_o)\sqrt{\phi}$ . Thus, the polymer coil's characteristic time of motion, $\phi$, is equal to $b^2 / (a - \mu_o)^2$.

Figure 7.3 shows a typical flow curve for a dilute solution of a high molecular weight polymer. The Bueche Equation was used to fit the data and determine the solution viscosity in the limit of very low shear rates or the "zero" shear solution viscosity.

**Intrinsic Viscosity**

At this point in the experimentation the "zero" shear viscosities of a set of polymer solutions having known polymer concentrations have been determined using the capillary viscometer and the data analysis described above. The intrinsic viscosity of the polymer in the given solvent can be now determined by producing a Huggins-Kramer plot.

The specific viscosity, $\eta_{sp} = (\eta - \mu_o) / \mu_o$, is related to the fluid viscosity increase due to all polymer solute molecules. The reduced viscosity, $\eta_{red} = \eta_{sp} / c$, is the fluid viscosity increase per unit of polymer solute concentration, c. The intrinsic viscosity, $\eta_{intr}$, is the limit of the reduced viscosity as the polymer solute concentration approaches zero. The intrinsic viscosity is also the limit of the

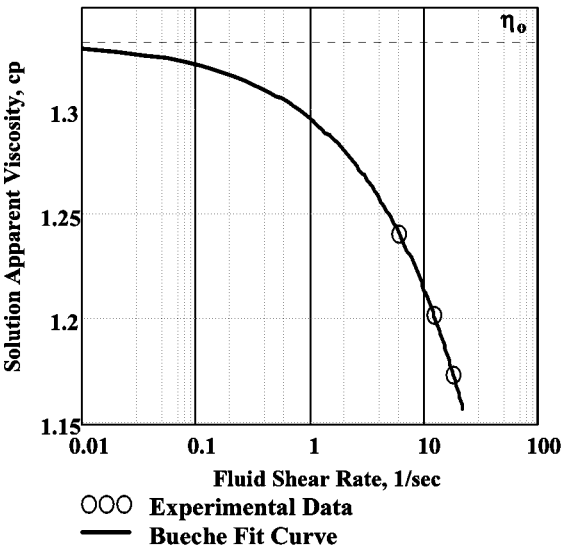


**Figure 7.3**. Typical Polymer Solution Flow Curve

inherent viscosity, $\ln(\eta_o / \mu_o)/c$, as the solution polymer concentration approaches zero.

$$\eta_{intr} = \lim_{c->0} \frac{\eta_{red}}{c} = \lim_{c->0} \frac{\ln(\eta_o / \mu_0)}{c}$$

Extrapolation to zero polymer concentration is intended to eliminate polymer intermolecular interactions. The plots used to find the intrinsic viscosity are called the Huggins plot ( $\eta_{red}$ vs. c ) and the Kraemer plot ( $\ln[\eta_o/\mu_o]/c$ vs. c ). As shown in Figure 7.4, the curves of both plots should be linear and have a common intercept that is the intrinsic viscosity, $\eta_{intr}$.

The intrinsic viscosity is the volume of polymer coils that would exist for a given mass of polymer dissolved in a solution. Usually the intrinsic viscosity is expressed in units of deciliters (dL) of coil volume per gram (g)of polymer. High molecular weight, water soluble, polymers usually have intrinsic viscosities greater than 10 dL/g and molecular weights, M, greater than $10^6$ g/mole. Thus, each polymer coil volume is mostly composed of solvent. Each coil occupies a volume, $V_{coil}$, equal to $\eta_{intr}$ M / $N_A$ where $N_A$ is Avogadro's Number.

The coil volume is directly proportional to the product of the intrinsic viscosity and the polymer molecular weight. Both the shear and extension rheological properties of polymer solutions are greatly affected by both the polymer coil volume and the fraction of solution occupied by all the polymer coils. When the polymer mass concentration, c, is approximately equal to $1/\eta_{intr}$, then all the solution volume is occupied by polymer coils. The polymer concentration at this condition is called the critical or overlap concentration, $c_{star}$. Solutions having polymer concentrations much less than $c_{star}$ are considered dilute because at these solution conditions each polymer coil acts independently of all other polymer coils in the solution.

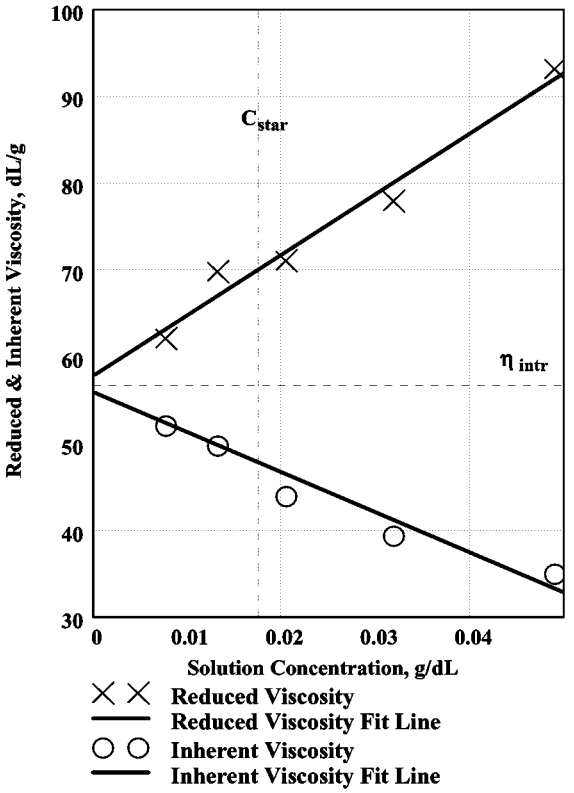


**Figure 7.4.** Typical Huggins-Kramer Plot

**Intrinsic Viscosities At Elevated Temperatures**

Intrinsic viscosity data have been collected and analyzed by the methods described above for several polymer-solvent systems at various temperatures. A commercially available poly(acrylamide), Alcoflood 1285[4], has been a focus of the efforts for use as a basis of comparison. Figure 7.5 shows Huggins and Kraemer plots for 0.514 M NaCl aqueous solutions (3.0 wt. % brine)

of Alcoflood 1285 polymer at three temperatures. For this polymer - solvent system the intrinsic viscosity increases with increasing temperature. This same trend has been reported by Dey and Laik for a similar poly(acrylamide) in 3% brine.[5] This type of intrinsic viscosity versus temperature behavior would favor more efficient flooding because polymer coil size would increase as a flooding solution is elevated in temperature after being injected into a reservoir. Any increase in polymer coil size reduces the displacement fluid's mobility and thus improves sweep performance during reservoir flooding.

## CONCLUSION

In Chapter 8 intrinsic viscosity measurements made at elevated temperatures will be compared with theory based on the work of Flory and Fixman for predicting intrinsic viscosity as a function of temperature.

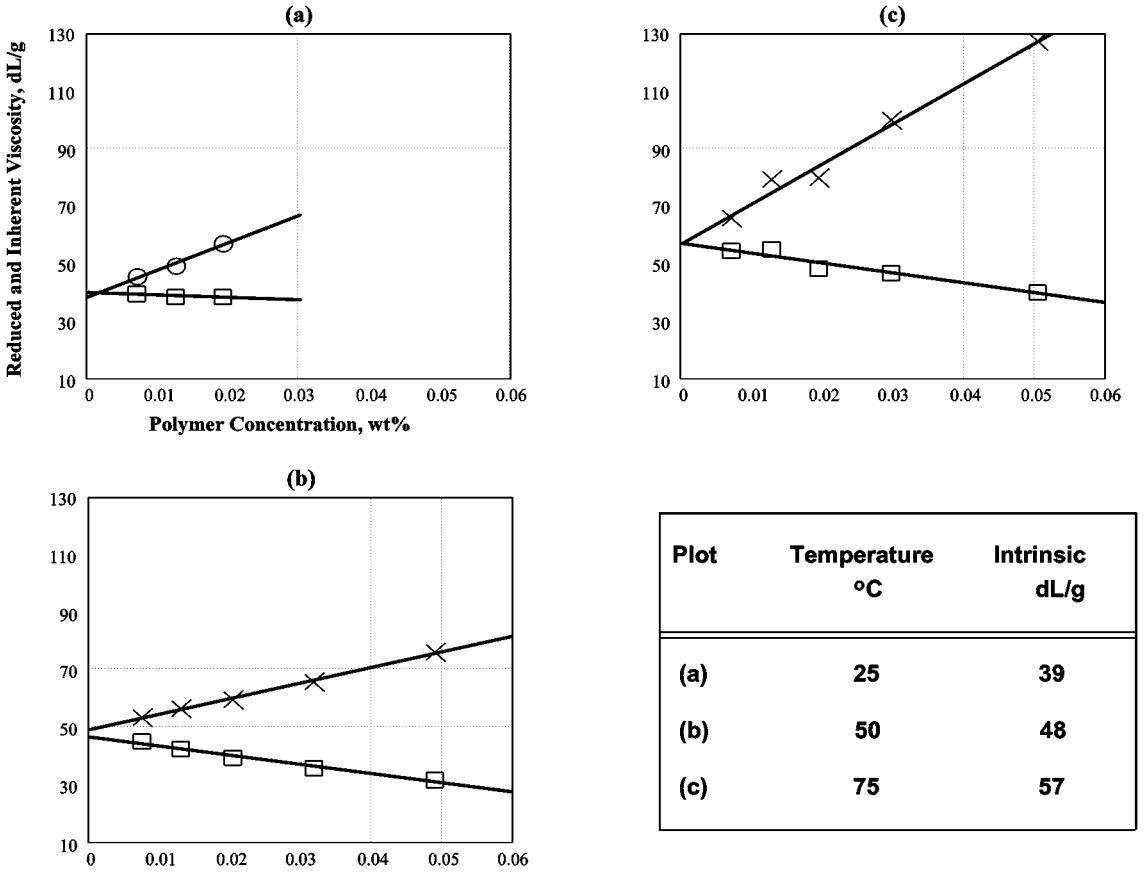


| Plot | Temperature °C | Intrinsic dL/g |
|---|---|---|
| (a) | 25 | 39 |
| (b) | 50 | 48 |
| (c) | 75 | 57 |

**Figure 7.5**. Huggins-Kraemer Plots of of Alcoflood 1285 in 0.514 M NaCl at 25, 50 & 75 °C.

**Nomenclature**

| Symbol | Description |
|---|---|
| a | constant used to determine $\phi$ |
| A | intercept of transducer calibration |
| b | slope of linearized Bueche relationship |
| B | slope of transducer calibration |
| c | solution polymer concentration, wt% |
| $c_{star}$ | polymer coil critical overlap concentration |
| L | capillary length |
| M | polymer molecular weight |
| $N_A$ | Avogadro's number |
| Q | volumetric flow rate |
| R | capillary inside radius |
| t | time |
| $t_{start}$ | time at which data acquisition begins |
| V | voltage |
| $V_{coil}$ | volume occupied by a polymer coil in solution |
| $V_{final}$ | final steady state voltage signal |
| $V_{start}$ | voltage at time $t_{start}$ |
| $\dot{\gamma}$ | shear rate at the capillary wall |
| $\Delta P$ | pressure drop across capillary |
| $\eta$ | apparent viscosity |
| $\eta_{intr}$ | intrinsic viscosity |
| $\eta_o$ | solution zero shear viscosity |

| | |
|---|---|
| $\eta_{red}$ | reduced viscosity |
| $\eta_{sp}$ | specific viscosity |
| $\lambda$ | constant proportional to instrument response time |
| $\mu_o$ | Newtonian solvent viscosity |
| $\phi$ | polymer characteristic time $\phi$ |

**REFERENCES**


1. Press, W. H., Flannery, B. P., Teukolsky, S. A., and Vetterling, W. T., *Numerical Recipes*; Cambridge University Press: New York (1986).

2. Bird, R. B., Stuart, W. E., Lightfoot, E. N., *Transport Phenomena*; John Wiley & Sons: New York (1960).

3. Bueche, F. *J. Chem. Phys.*, *22*, 1570 (1954).

4. Alcoflood 1285, a high molecular weight poly(acrylamide) with an anionic content of 25 mole percent from Ciba Specialty Chemicals Water Treatments, Inc., Suffolk, VA.

5. Dey, N. C. and Laik, S. *J. Inst. Eng. (India), Part CH* , *66(2)*, 22-24 (1986).

# CHAPTER 8. POLYMER SOLUTION EXTENSIONAL RHEOLOGICAL STUDIES

## INTRODUCTION

### Previous Results

As explained in previous reports [1, 2], the mobility of a polymer solution flowing through a porous media is a function of the fluid's resistance to extensional strains. These strains are developed when the fluid velocity varies in the direction of flow. These velocity gradients in the flow direction result from the non-uniform size flow channels found within any porous media. Fluid velocity acceleration and deceleration within the pore channels produce the forces to extend and compress the polymer coils found within the solution. Energy is needed to deform the polymer coils as they pass through the porous media and this energy is removed from the flow field causing a decrease in fluid mobility.

Several polymer solutions have been characterized for extensional flow resistance using a screen extensional rheometer (SER). Two parameters to quantify solution extensional rheology have been developed using the SER. These parameters are the fluid flow rate when the polymer coils start to extend, $Q_{yield}$ , and $\eta_c$, the polymer coil viscosity. Fluid mobility decreases as the coil viscosity increases. When using dilute polymer solutions to enhance oil recovery from reservoirs, low values of $Q_{yield}$ and high values of $\eta_c$ are desired to improve oil recovery efficiency.

With an estimation of the hydrodynamic volumes known for each polymer, a plot of coil viscosity versus hydrodynamic volume was generated and is shown in Figure 8.1. Figure 8.1 also includes a plot of the yield extension rate for each polymer versus hydrodynamic volume. As can be seen in Figure 8.1, both plots were fit to a straight line.

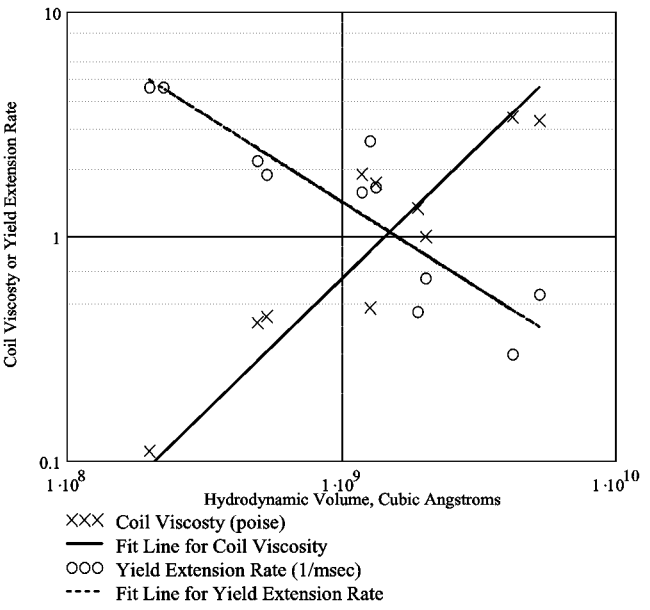


**Figure 8.1.** Polymer Extensional Properties versus Coil Hydrodynamic Volume

Both $Q_{yield}$ and $\eta_c$ appear to be dependent upon the polymer coil's hydrodynamic volume, $V_c$. When $V_c$ increases, the coil viscosity, $\eta_c$, increases and the yield flow rate, $Q_{yield}$, decreases. It was estimated that

$$\eta_c \approx V_c^{1.18} \quad \text{and} \quad Q_{yield} \approx V_c^{-0.80}$$

Coil volume, $V_c$, in Angstrom$^3$, can be approximated as

$V_c \cong \frac{125\pi}{6}(M\ \eta_{intr})$ where M and $\eta_{intr}$ are the polymer's molecular weight in grams per mole and intrinsic viscosity in deciliters per gram, respectively.

Thus to have improved oil recovery when flooding reservoirs with polymer solutions, larger polymer coil hydrodynamic volumes are needed. Coil hydrodynamic volumes can be estimated from intrinsic viscosity and polymer molecular weight measurements.

## EXPERIMENTAL

### Polymer Coil Hydrodynamic Volume

A polymer coil's hydrodynamic volume, $V_c$, is proportional to the product of the polymer's intrinsic viscosity, $\eta_{intr}$, and its molecular weight, M. To minimize cost, a minimum of polymer concentration is desired and therefore economics dictate that the polymers used in oil reservoir flooding should have both high molecular weights and large intrinsic viscosities.

$$\eta_c \approx V_c^{1.18} \approx \left(M\,\eta_{intr}\right)^{1.18} \qquad Q_{yield} \approx V_c^{-0.80} \approx \left(M\,\eta_{intr}\right)^{-0.80}$$

A polymer coil's hydrodynamic volume or intrinsic viscosity depends upon the degree of solvent-polymer thermodynamic interaction. Favorable solvent-polymer thermodynamic interaction increases polymer coil hydrodynamic volume or intrinsic viscosity. When the solvent-polymer interactions are not favorable, the polymer coil volume decreases. With very unfavorable solvent-polymer interactions, the polymer coil will completely collapse and will no longer be soluble in the solvent. Solvent-polymer thermodynamic interaction depends upon polymer molecular structure and concentration, solvent molecular structure, and solution temperature [3].

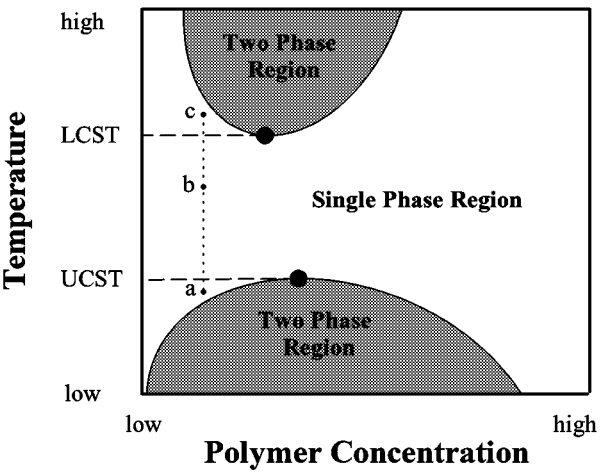


**Figure 8.2** Polymer Solution Phase Diagram

### Intrinsic Viscosity Dependence Upon Solution Temperature

Figure 8.2 shows a phase diagram for a typical polymer solution. Most polymers will have both a lower critical solution temperature, LCST, and a upper critical solution temperature, UCST. At temperatures bove the LCST or at temperatures below the UCST, phase separation can occur. At solution temperatures between the UCST and LCST, a single phase region exists. The two phase regions are separated from the single phase region by boundary curves (binodial curves). Polymer-solvent mixtures inside a binodial curve separate into two liquid phases having compositions on the binodial curve. The LCST usually occurs at about 0.8 of the pure solvent gas-liquid critical temperature [4]. Using this estimation technique, the LCST for water is expected to be about 518 °K or 245 °C.

For dilute polymer solutions at a low temperature (point "a" in Figure 8.2), the polymer coils in the solution usually increase in hydrodynamic volume as the temperature increases to temperatures

greater than the lower two phase critical solution temperature. As the solution temperature continues to increase, the polymer coil volume eventually reaches a maximum (point "b") and thereafter decreases in volume as the solution temperature ( point "c") begins to approach the upper critical temperature.

Several theories have been proposed to explain the relationship between a polymer coil's hydrodynamic volume and solution temperature. Most theories are based on the work of Flory in which a theta temperature, $\theta$ , is defined as the critical miscibility temperature for a given solvent-polymer system in the limit of infinite polymer molecular weight [5]. At theta conditions the excess chemical potential of mixing is zero. If the heat of polymer-solvent mixing is endothermic, an increase in solution temperature (to temperatures greater than the theta temperature) will increase polymer coil hydrodynamic volume. If the heat of polymer-solvent mixing is exothermic, a decrease in solution temperature (to temperatures less than the theta temperature) will increase polymer coil hydrodynamic volume.

**Flory Theory**

Theoretical relationships of Paul Flory showed that a polymer coil volume expansion, $\alpha$, was a function of solution absolute temperature, T, and the number of polymer segments, N.

$$\alpha^5 - \alpha^3 \approx \sqrt{N}\left(1 - \frac{\theta}{T}\right) \qquad \text{Flory Equation}$$

The expansion factor , $\alpha$, is the cube root of the ratio of the intrinsic viscosity, $\eta_{intr}$ , to intrinsic viscosity at the theta temperature, $\eta_\theta$ . For high molecular weight polymers that have a large number of segments the $\alpha^3$ term can be neglected. After inserting $\left(\eta_{intr} / \eta_\theta\right)^{1/3}$ for $\alpha$, the simplified equation becomes linear.

$$\left(\frac{\eta_{intr}}{\eta_\theta}\right)^{\frac{5}{3}} \approx \sqrt{N}\left(1 - \frac{\theta}{T}\right) \qquad \text{Simpilified Flory Equation}$$

$$\left(\eta_{intr}\right)^{\frac{5}{3}} \cong \sqrt{N}\left(\eta_\theta\right)^{\frac{5}{3}} - \sqrt{N}\left(\eta_\theta\right)^{\frac{5}{3}}\theta\left(\frac{1}{T}\right) \qquad \text{Linear Equation}$$

The equation above indicates that a plot of $\left(\eta_{intr}\right)^{\frac{5}{3}}$ versus $\frac{1}{T}$ should yield data points that fall on a straight line. The intercept, a, and slope, b, of the line should be $\sqrt{N}\left(\eta_\theta\right)^{\frac{5}{3}}$ and $\sqrt{N}\left(\eta_\theta\right)^{\frac{5}{3}}\theta$, respectively. The theta temperature, $\theta$ , is equal to -b/a. If the number of polymer segments, N, can has been estimated [8] as the polymer molecular weight, M, divided by 100 times monomer molecular weight, $M_o$, then the intrinsic viscosity at theta conditions, $\eta_\theta$ , is equal to $\left(\frac{a\sqrt{100\,M_o}}{\sqrt{M}}\right)^{\frac{3}{5}}$.

Figure 8.3 shows the linear form of the Flory plot of two partially hydrolyzed polyacrylamide polymers in brine solution, Alcoflood 1285 (Ciba Specialty Chemicals PLC) in 0.514 molar NaCl and Pusher 700 (Dow Chemical Co.) in 3 wt. % NaCl. The random degree of hydrolysis for both polymers is between 25 and 30%. The molecular weights for the Alcoflood 1285 and Pusher 700 polymers are about 20 million and 5 million, respectively. The monomer molecular weight, $M_o$, for both polymers is 71 grams per mole. Data for the Pusher 700 polymer was taken from the literature [8].

Table 8. gives the Flory parameters that were calculated from the plots given in Figure 3.

**Table 8.1**: Flory Parameters

| Para meter | Units | Pusher 700 | Alcoflood 1285 |
|---|---|---|---|
| M | g/mole x $10^6$ | 5 | 20 |
| $M_o$ | g/mole | 71 | 71 |
| N | | 700 | 2800 |
| $\eta_\theta$ | dL/g | 5.0 | 11.7 |
| $\theta$ | °K | 257 | 226 |

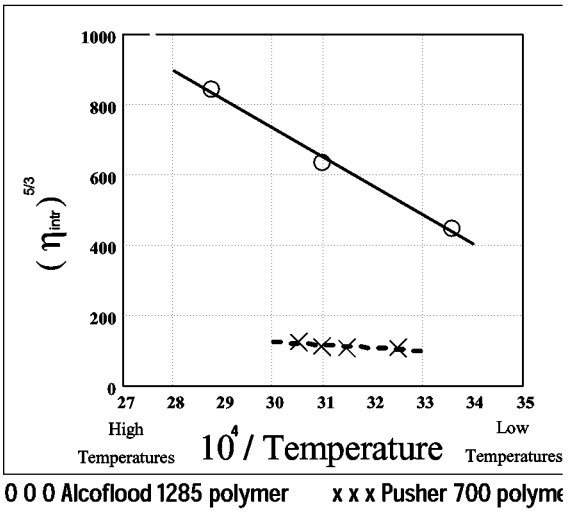


**Figure 8.3** : Flory Plots for Acrylamide Polymers

**Fixman Theory**

Fixman's theory[6] used Flory's concepts to describe the dependence of intrinsic viscosity on temperature. This theory can be expressed as shown below [7].

$$d\eta_{intr} = \lambda\, \eta_\theta\, dT + \frac{\theta}{T}\left(\frac{\eta_{intr} - \eta_\theta}{T - \theta}\right) dT \qquad \text{Fixman Equation}$$

The fist term on the right side of the above equation is related to the partial change in polymer coil volume or intrinsic viscosity, $\eta_{intr}$, with respect to a change in temperature, T, if the coil were under theta conditions (coil unperturbed by solvent). The last term of the above equation is related to the partial change in polymer coil volume with respect to a change in temperature that is due to solvent-polymer thermodynamic interaction. Two parameters are used in the Fixman equation: $\lambda$ is the fraction of unperturbed coil volume change with respect to a temperature change and, $\eta_\theta$ is the intrinsic viscosity at theta conditions. For a given solvent-polymer system both $\lambda$ and $\eta_\theta$ are considered constant; i.e., they do not vary with temperature.

The Fixman equation is a linear first order ordinary differential equation that can be solved using the integrating factor technique to give

$$\eta_{intr} = \lambda\, \eta_\theta\, (T - \theta)\left(1 + \frac{\theta}{T}\ln(T - \theta)\right) + \frac{\eta_\theta\, \theta}{T} + \left(\frac{T - \theta}{T}\right) k$$

where k is an integration constant and can be evaluated if the intrinsic viscosity, $\eta_{intr\_ref}$, at some reference temperature, $T_{ref,}$ is known.

$$k = \frac{\eta_{intr\_ref}}{\lambda\,\eta_\theta\,(T_{ref}-\theta)\left(1+\frac{\theta}{T_{ref}}\ln(T_{ref}-\theta)\right)+\frac{\eta_\theta\,\theta}{T_{ref}}+\left(\frac{T_{ref}-\theta}{T_{ref}}\right)}$$

As an example, the above equations were used to generate Figure 8.4. This figure shows intrinsic viscosity estimates for a 4.1 million molecular weight poly(ethylene)oxide (PEO) in deionized water between 2C (275 °K) and 97C (370 °K). The values of the parameters used for this estimate were $\theta$ = 371 °K, $\eta_\theta$ = 3.3 dL/g, $\lambda$ = -0.0014 °K$^{-1}$, $T_{ref}$ = 295 °K and $\eta_{intr\_ref}$ = 18.6 dL/g. Note that for this solution the intrinsic viscosity decreases as the temperature increases from room conditions.

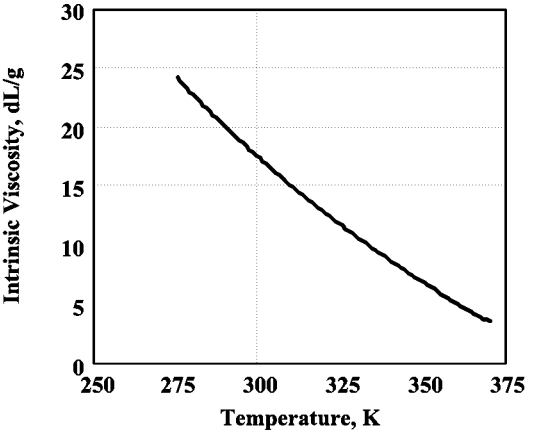


**Figure 8.4.** Intrinsic Viscosity vs. Temperature Function for 4.1 million PEO in water

**Polymer Solution Temperatures During Reservoir Flooding**

After injection, a polymer solution increases in temperature and rapidly approaches the reservoir temperature. Usually reservoir temperatures are much above room temperature conditions. Ideally, the flooding solution intrinsic viscosity should remain constant or preferably increase as it leaves the injection well and thereafter heats up to the reservoir temperature. This advantageous property would insure that the displacing fluid mobility would not increase due to a reduction in polymer coil hydrodynamic volume as the solution migrates into the reservoir. The polyacrylamide polymer solutions of Figure 8.3 have the temperature response that is favorable for oil reservoir flooding; however, the PEO solution shown in Figure 8.4 has the opposite behavior needed for good displacing fluid mobility control during reservoir flooding.

**Polymer Solution Rheology at Elevated Temperatures**

All previous polymer solution tests for rheology characteristics using the Screen Extensional Rheometer, SER, were performed at room temperature conditions (~22C). However, the temperatures of oil reservoirs are always higher than room conditions. Therefore, to project polymer solution mobility in reservoirs at elevated temperatures, the SER is being modified to determine the dependence of polymer solution extensional flow properties as a function of temperature.

A Tamson model TV 4000 bath has been used to submerge the SER in hot aqueous fluid. Initial experiments reveled that submerging the SER required additional modifications to the SER. The pressure transducers required special standoffs to thermally isolate them from the hot bath fluid. Also, the stainless steel tubing that leads polymer solution into the SER was lengthened to provide ample time for heat transfer from the bath fluid to the polymer solution in the tube before being forced through the SER. This modification assured that the polymer solution temperature was at the bath fluid temperature before entering the SER. SER studies were performed at elevated temperatures on a poly(ethylene oxide) homopolymer and several polyacrylamide based copolymers.

***Poly(ethylene oxide) Solutions***

Aqueous solution of poly(ethylene oxide) having a molecular weight of 4.1 x $10^6$ g/mole were forced through the SER at 60°C (333°K). The polymer solution intrinsic viscosity at 60°C was made using Figure 8.4. The estimated intrinsic viscosity at 60°C was 9.96 dL/g. The results were then compared to the previously reported PEO data that was taken at 22°C (295°K). See Table 8.2 shown below.

**Table 8.2.** PEO Solution Properties

| Polymer | Solvent | Temperature (C) | Intrinsic Viscosity (dL/g) | $Q_{yield}$ (mL/min) | $\eta_c$ (poise) |
|---|---|---|---|---|---|
| PEO 4.1M | DI Water | 22 | 18.6+ | 12 | 3.27 |
| PEO 4.1M | DI Water | 60 | 9.96* | 10 | 1.28 |

* Estimated using Figure 4 + Measured using the Contraves Low Shear 30 rheometer

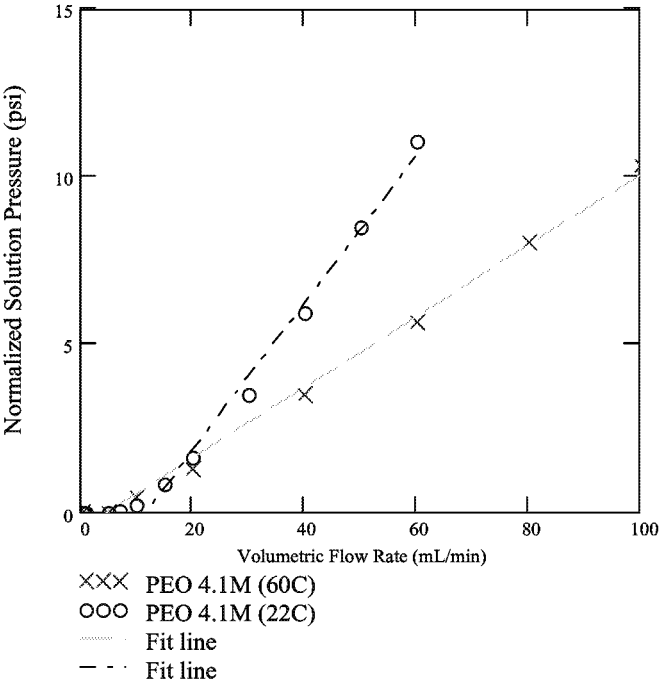


**Figure 8.5.** PEO Solution SER Results

Figure 8.5 shows a plot of the Normalized Solution Pressure versus volumetric flow rate for the polymer solution at both temperatures. As can be seen from the plot a higher pressure can be attained at lower flow rates when the solution temperature is 22°C. The coil viscosity is larger at a solution temperature of 22C, 3.27 poise, than that of the solution at 60°C, 1.28 poise. Thus an elevation of solution temperature above room conditions resulted in the coil viscosity being lowered by 61%. This result is in concert with Figure 8.1, shown above, which predicts a decrease in coil viscosity that would be proportional to the ratios of the intrinsic viscosities taken to a power of 1.18. In other words, experimentation suggests that $\eta_{c60C} = \eta_{c22C} (\eta_{intr60C} / \eta_{intr22C})^{1.18} = 3.27 (9.96 / 18.6)^{1.18} = 3.27(0.48) = 1.56$ poise. This expected value is close to that experimentally determined, 1.28 poise. The yield flow rate was slightly lower at 60C with a value of 10 mL/min. This is not in agreement with theoretical predictions which suggest that $Q_{yield60C} = Q_{yield22C} (\eta_{intr60C} / \eta_{intr22C})^{-0.80} = 12 (9.96 / 18.6)^{-0.80} = 12 (1.65) = 20$ mL/min. This expected value is larger than experimentally determined, 12 mL/min.

***Polyacrylamide Solutions***

Dilute solutions of three polyacrylamide copolymers were studied using the SER at 25 and 50 °C. Two solution were made using commercially available [9] hydrolyzed polyacrylamides, Alcoflood 1285 and Alcoflood 1235. Both polymers are hydrolyzed to 25 to 30 % but are of different

molecular weights. The third solution was made using NaAMB-10-2, a copolymer composed of 10 mole % of a sodium salt of a acid monomer, 3-acrylamido-3-methylbutanoic acid, and 90 mole % of acrylamide monomer [10]. All solutions were made using 0.514 molar NaCl aqueous solvent. Figure 8.6 shows a plot of the Normalized Solution Pressure versus volumetric flow rate for the polymer solutions at both temperatures. Table 8.3 gives information on polymer properties and the results from the SER studies, coil viscosities and yield extension rates.

**Table 8.3.** Acrylamide Copolymer Properties and Results from SER Studies

| Polymer | Temp., °C | Mol. Wt., grams/mole x $10^{-6}$ | Intrinsic Viscosity, dL/g | Coil Volume, $\mathring{A}^3$ x $10^{-10}$ | Coil Viscosity, poise | Yield Rate, 1/msec |
|---|---|---|---|---|---|---|
| Alcoflood 1285 | 25 | 20 | 39 | 5.1 | 2.29 | 0.23 |
| Alcoflood 1285 | 50 | 20 | 48 | 6.3 | 0.82 | 0.18 |
| Alcoflood 1235 | 25 | 12 | 19 | 1.5 | 0.96 | 0.69 |
| Alcoflood 1235 | 50 | 12 | 20 | 1.6 | 0.45 | 0.41 |
| NaAMB-10-2 | 25 | 13 | 23 | 2.0 | 0.86 | 0.28 |
| NaAMB-10-2 | 50 | 13 | 21 | 1.8 | 0.53 | 0.55 |

As shown in Table 8.3, the intrinsic viscosities of both Alcoflood polymer solutions increased as the temperature was increased from 25 to 50 °C. The increase was much greater for the higher molecular weight hydrolyzed copolymer, Alcoflood 1285. The NaAMB-10-2 solution slightly decreased in intrinsic viscosity as the temperature was elevated. All the copolymer coil viscosities decreased with increasing temperature. Both hydrolyzed copolymers had yield extension rates that decreased with increasing solution temperature, however, the NaAMB-10-2 copolymer's yield extension rate increased with increased temperature.

## CONCLUSIONS

The intrinsic viscosity dependence on solution temperature for two high molecular weight polyacrylimide copolymers in brine solutions was found to follow a simplified form of Flory's theoretical relationship. The intrinsic viscosities increased as the solution temperature increased from 25 to 75 °C. Theta temperatures and intrinsic viscosities at theta conditions were determined for both polymer-solvent systems. In contrast, the intrinsic viscosity of a poly(ethylene oxide) aqueous solution was found to decease with elevated temperatures.

Studies involving measurement of the extensional rheological properties of high molecular weight poly(ethylene)oxide and acrylamide copolymer aqueous solution at elevated temperature using the screen extensional rheometer gave results that, in general, confirmed what was predicted from theoretical relationships. At higher temperatures, a polymer solution's mobility significantly increased. Thus, at higher temperatures these polymers would be less efficient at sweeping oil from a reservoir.

This rheology study accentuated the importance of developing polymer solutions that increase in intrinsic viscosity when fluid temperatures are elevated above room conditions and also maintain

high coil viscosities. Ideally it is desired that a polymer flooding solution's intrinsic viscosity remain constant or preferably increase as it leaves the injection well and thereafter heats up to the reservoir temperature. This advantageous polymer solution property would insure that fluid mobility control would not be diminished as the solution migrates into and through a hot reservoir and thereby would improve sweep efficiency and oil recovery.

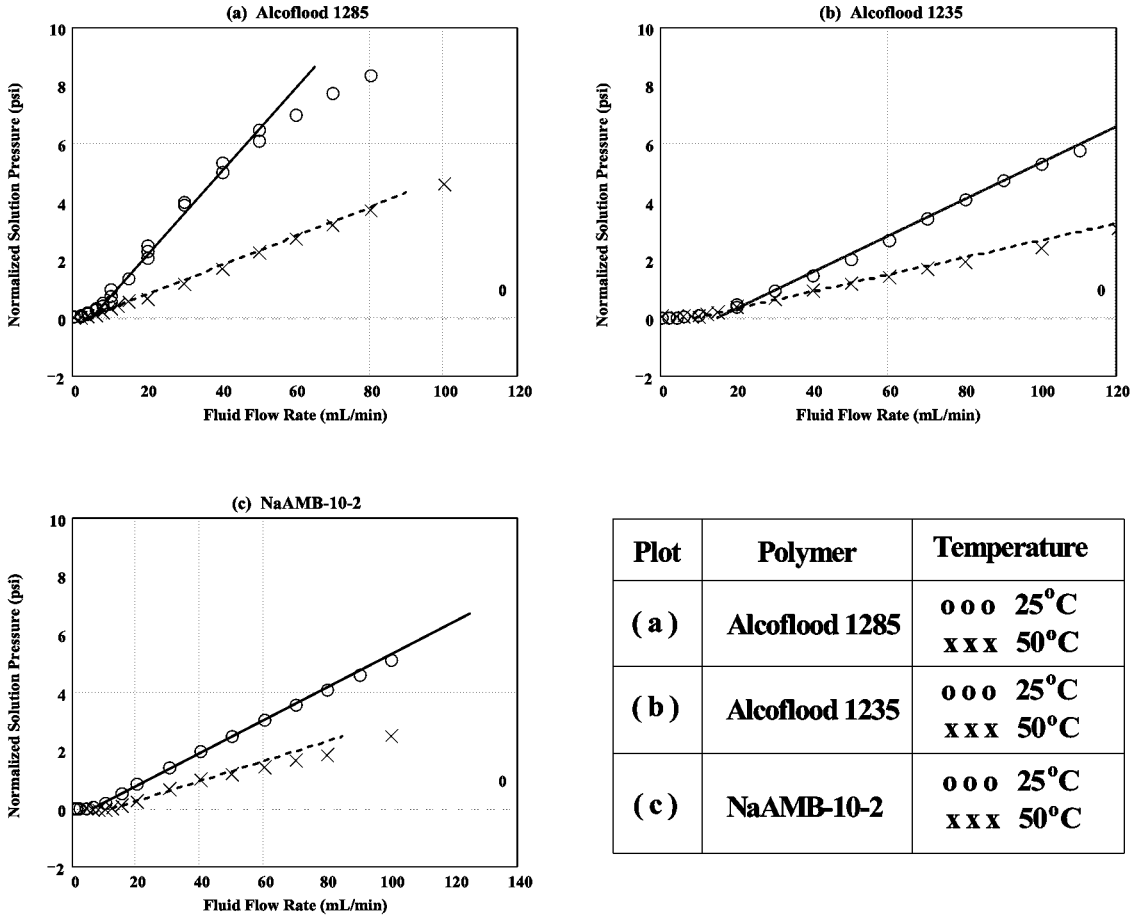


| Plot | Polymer | Temperature |
|---|---|---|
| (a) | Alcoflood 1285 | ooo 25°C<br>xxx 50°C |
| (b) | Alcoflood 1235 | ooo 25°C<br>xxx 50°C |
| (c) | NaAMB-10-2 | ooo 25°C<br>xxx 50°C |

**Figure 8.6.** Acrylamide Copolymer Solution SER Results

**Nomenclature**

| Symbol | Description |
|---|---|
| k | integration constant used in the Fixman equation |
| $Q_{yield}$ | fluid volumetric flow rate at which polymer coils start to extend |
| M | polymer molecular weight |
| Mo | monomer molecular weight |

| | |
|---|---|
| $N$ | number of flexible segments in a polymer molecule |
| $T$ | absolute temperature |
| $T_{ref}$ | reference temperature used to determine integration constant c |
| $V_c$ | polymer coil hydrodynamic volume |
| $\eta_c$ | polymer coil viscosity |
| $\eta_{intr}$ | intrinsic viscosity |
| $\eta_{intr\_ref}$ | reference intrinsic viscosity used to determine integration constant c |
| $\eta_\theta$ | intrinsic viscosity at theta conditions (coil unperturbed conditions) |
| $\theta$ | theta temperature ( temperature corresponding to coil unperturbed conditions) |
| $\lambda$ | fraction of unperturbed coil volume change with respect to a temperature change |

## REFERENCES


1. McCormick, C. L. and R. D. Hester, *Responsive Copolymers for Enhanced Petroleum Recovery, Annual Report,* June 2000 (DOE/BC/15111-1).

2. McCormick, C. L. and R. D. Hester, *Responsive Copolymers for Enhanced Petroleum Recovery, Annual Report,* Feburary 2001 (DOE/BC/15111-2).

3. Brandrup, J. and E. H. Immergut, *Polymer Handbook, Second Edition*, John Wiley & Sons, N.Y. , IV-157, (1975).

4. Sanchez, I. C. , *Encyclopedia of Physical Science and Technology, Vol. II*, Ed. By Meyers, R. A., Academic Press (1987).

5. Flory, P. J., *Principles of Polymer Chemistry*, Cornell University Press, Ithaca, N. Y., 425 (1953).

6. Fixman, M., *J. Chem. Phys.,* 36, 3123 (1962).

7. Gregory, P., M. B. Huglin, M. K. H. Khorasani and P. M. Sasia, *British Polymer J.,* 20, 1-8 (1988).

8. Dey, N. C. and Laik, S. *J. Inst. Eng. (India), Part CH , 66(2)*, 22-24 (1986).

9. Ciba Speciality Chemicals Water Treatments, Inc., Suffolk, VA.

10. McCormick, C. L., & K. P. Blackmon, Patent No. 4,649,183 (1987)